



- and Shapiro, S.D. 1997. Requirement for macrophage elastase for cigarette smoke-induced emphysema in mice. *Science*. 277:2002-2004.
8. Zheng, T., et al. 2000. Inducible targeting of IL-13 to the adult lung causes matrix metalloproteinase- and cathepsin-dependent emphysema. *J. Clin. Invest.* 106:1081-1093.
9. Horvath, I., et al. 2001. "Haemoxigenase-1 induction and exhaled markers of oxidative stress in lung diseases", summary of the ERS Research Seminar in Budapest, Hungary, September, 1999. *Eur. Respir. J.* 18:420-430.
10. MacNee, W., and Rahman, I. 2001. Is oxidative stress central to the pathogenesis of chronic obstructive pulmonary disease? *Trends Mol. Med.* 7:55-62.
11. Li, J., et al. 2003. Signaling intermediates required for NF- κ B activation and IL-8 expression in CF bronchial epithelial cells. *Am. J. Physiol. Lung Cell Mol. Physiol.* 284:L307-L315.
12. Cho, H.Y., et al. 2002. Linkage analysis of susceptibility to hyperoxia. Nrf2 is a candidate gene. *Am. J. Respir. Cell Mol. Biol.* 26:42-51.
13. Nguyen, T., Sherratt, P.J., and Pickett, C.B. 2002. Regulatory mechanisms controlling gene expression mediated by the antioxidant response element. *Annu. Rev. Pharmacol. Toxicol.* 17:17.
14. Itoh, K., et al. 1997. An Nrf2/small Maf heterodimer mediates the induction of phase II detoxifying enzyme genes through antioxidant response elements. *Biochem. Biophys. Res. Commun.* 236:313-322.
15. Cavarra, B., et al. 2001. Effects of cigarette smoke in mice with different levels of alpha(1)-proteinase inhibitor and sensitivity to oxidants. *Am. J. Respir. Crit. Care Med.* 164:886-890.
16. Aoshiba, K., Yokohori, N., and Nagai, A. 2003. Alveolar wall apoptosis causes lung destruction and emphysematous changes. *Am. J. Respir. Cell Mol. Biol.* 28:555-562.
17. Finkelstein, R., Fraser, R.S., Ghezzi, H., and Cosio, M.G. 1995. Alveolar inflammation and its relation to emphysema in smokers. *Am. J. Respir. Crit. Care Med.* 152:1666-1672.
18. Trevani, A.S., et al. 1996. Neutrophil apoptosis induced by proteolytic enzymes. *Lab. Invest.* 74:711-721.
19. Segura-Valdez, L., et al. 2000. Upregulation of gelatinases A and B, collagenases 1 and 2, and increased parenchymal cell death in COPD. *Chest.* 117:684-694.
20. Kasai, H. 1997. Analysis of a form of oxidative DNA damage, 8-hydroxy-2'-deoxyguanosine, as a marker of cellular oxidative stress during carcinogenesis. *Mutat. Res.* 387:147-163.
21. Cho, H.Y., et al. 2002. Role of Nrf2 in protection against hyperoxic lung injury in mice. *Am. J. Respir. Cell Mol. Biol.* 26:175-182.
22. Chan, K., and Kan, Y.W. 1999. Nrf2 is essential for protection against acute pulmonary injury in mice. *Proc. Natl. Acad. Sci. U. S. A.* 96:12731-12736.
23. Dhakshinamoorthy, S., and Jaiswal, A.K. 2000. Small maf (MafG and MafK) proteins negatively regulate antioxidant response element-mediated expression and antioxidant induction of the NAD(P)H:Quinone oxidoreductase1 gene. *J. Biol. Chem.* 275:40134-40141.
24. He, C.H., et al. 2001. Identification of activating transcription factor 4 (ATF4) as an Nrf2-interacting protein. Implication for heme oxygenase-1 gene regulation. *J. Biol. Chem.* 276:20858-20865.
25. Das, K.C., and White, C.W. 2002. Redox systems of the cell: possible links and implications. *Proc. Natl. Acad. Sci. U. S. A.* 99:9617-9618.
26. Casagrande, S., et al. 2002. Glutathionylation of human thioredoxin: a possible crosstalk between the glutathione and thioredoxin systems. *Proc. Natl. Acad. Sci. U. S. A.* 99:9745-9749.
27. Sies, H., and Arnt, G.B. 2000. Interaction of peroxynitrite with selenoproteins and glutathione peroxidase mimics. *Free Radic. Biol. Med.* 28:1451-1455.
28. Nordberg, J., and Arner, E.S. 2001. Reactive oxygen species, antioxidants, and the mammalian thioredoxin system. *Free Radic. Biol. Med.* 31:1287-1312.
29. Kim, P.M., and Wells, P.G. 1996. Genoprotection by UDP-glucuronosyltransferases in peroxidase-dependent, reactive oxygen species-mediated micronucleus initiation by the carcinogens 4-(methylnitrosamino)-1-(3-pyridyl)-1-butanone and benzo[a]pyrene. *Cancer Res.* 56:1526-1532.
30. Engel, L.S., et al. 2002. Pooled analysis and meta-analysis of glutathione S-transferase M1 and bladder cancer: a HuGE review. *Am. J. Epidemiol.* 156:95-109.
31. Dinkova-Kostova, A.T., and Talalay, P. 2000. Persuasive evidence that quinone reductase type 1 (DT diaphorase) protects cells against the toxicity of electrophiles and reactive forms of oxygen. *Free Radic. Biol. Med.* 29:231-240.
32. Vogt, B.A., Alam, J., Croatt, A.J., Vercellotti, G.M., and Nath, K.A. 1995. Acquired resistance to acute oxidative stress. Possible role of heme oxygenase and ferritin. *Lab. Invest.* 72:474-483.
33. Brittenham, G.M., et al. 2000. Clinical consequences of new insights in the pathophysiology of disorders of iron and heme metabolism. *Hematology (Am. Soc. Hematol. Educ. Program)*. 39-50.
34. Folz, R.J., Abushama, A.M., and Suliman, H.B. 1999. Extracellular superoxide dismutase in the airways of transgenic mice reduces inflammation and attenuates lung toxicity following hyperoxia. *J. Clin. Invest.* 103:1055-1066.
35. Poller, W., et al. 1992. Mis-sense mutation of alpha 1-antichymotrypsin gene associated with chronic lung disease. *Lancet.* 339:1538.
36. Ramos-Gomez, M., et al. 2001. Sensitivity to carcinogenesis is increased and chemoprotective efficacy of enzyme inducers is lost in nrf2 transcription factor-deficient mice. *Proc. Natl. Acad. Sci. U. S. A.* 98:3410-3415.
37. Witschi, H., Espiritu, I., Maronpot, R.R., Pinkerton, K.B., and Jones, A.D. 1997. The carcinogenic potential of the gas phase of environmental tobacco smoke. *Carcinogenesis* 18:2035-2042.
38. Kasahara, Y., et al. 2000. Inhibition of VEGF receptors causes lung cell apoptosis and emphysema. *J. Clin. Invest.* 106:1311-1319.
39. Kasahara, Y., et al. 2001. Endothelial cell death and decreased expression of vascular endothelial growth factor and vascular endothelial growth factor receptor 2 in emphysema. *Am. J. Respir. Crit. Care Med.* 163:737-744.
40. Saltini, C., et al. 1984. Accurate quantification of cells recovered by bronchoalveolar lavage. *Am. Rev. Respir. Dis.* 130:650-658.
41. Tirumalai, R., Rajesh Kumar, T., Mai, K.H., and Biswal, S. 2002. Acrolein causes transcriptional induction of phase II genes by activation of Nrf2 in human lung type II epithelial (A549) cells. *Toxicol. Lett.* 132:27-36.
42. Thimmulappa, R.K., et al. 2002. Identification of Nrf2-regulated genes induced by the chemopreventive agent sulforaphane by oligonucleotide microarray. *Cancer Res.* 62:5196-5203.
43. Wasserman, W.W., and Fahl, W.B. 1997. Functional antioxidant responsive elements. *Proc. Natl. Acad. Sci. U. S. A.* 94:5361-5366.
44. Flohe, L., and Gunzler, W.A. 1984. Assays of glutathione peroxidase. *Meth. Enzymol.* 105:114-121.
45. Prochaska, H.J., and Santamaria, A.B. 1988. Direct measurement of NAD(P)H:quinone reductase from cells cultured in microtiter wells: a screening assay for anticarcinogenic enzyme inducers. *Anal. Biochem.* 169:328-336.
46. Chae, H.Z., Kang, S.W., and Rhee, S.G. 1999. Isoforms of mammalian peroxiredoxin that reduce peroxides in presence of thioredoxin. *Meth. Enzymol.* 300:219-226.
47. Lee, C.Y. 1982. Glucose-6-phosphate dehydrogenase from mouse. *Meth. Enzymol.* 89:252-257.
48. Carlberg, I., and Mannervik, B. 1985. Glutathione reductase. *Meth. Enzymol.* 113:484-490.

International Research Conference on Food, Nutrition, and Cancer

Transcription Factor Nrf2 Is Essential for Induction of NAD(P)H:Quinone Oxidoreductase 1, Glutathione S-Transferases, and Glutamate Cysteine Ligase by Broccoli Seeds and Isothiocyanates^{1,2}

Gail K. McWalter, Larry G. Higgins, Lesley I. McLellan, Colin J. Henderson, Lijiang Song,* Paul J. Thornalley,* Ken Itoh,[†] Masayuki Yamamoto,[†] and John D. Hayes³

Biomedical Research Centre, Ninewells Hospital and Medical School, University of Dundee, Dundee DD1 9SY, Scotland, United Kingdom; *Disease Mechanisms and Therapeutics Research Group, Department of Biological Sciences, University of Essex, Essex CO4 3SQ, United Kingdom; [†]Centre for Tsukuba Advanced Research Alliance and Institute of Basic Medical Sciences, University of Tsukuba, Tsukuba 305-8577, Japan

ABSTRACT Cruciferous vegetables contain glucosinolates that, after conversion to isothiocyanates (ITC), are capable of inducing cytoprotective genes. We examined whether broccoli seeds can elicit a chemoprotective response in mouse organs and rodent cell lines and investigated whether this response requires nuclear factor-erythroid 2 p45-related factor 2 (Nrf2). The seeds studied contained glucosinolate at 40 mmol/kg, of which 59% comprised glucoiberin, 19% sinigrin, 8% glucoraphanin, and 7% progoitrin. Dietary administration of broccoli seeds to *nrf2*^{+/+} and *nrf2*^{-/-} mice produced a ~1.5-fold increase in NAD(P)H:quinone oxidoreductase 1 (NQO1) and glutathione S-transferase (GST) activities in stomach, small intestine, and liver of wild-type mice but not in mutant mice; increased transferase activity was associated with elevated levels of GSTA1/2, GSTA3, and GSTM1/2 subunits. These seeds also increased significantly the level of glutamate cysteine ligase catalytic (GCLC) subunit in the stomach and the small intestine of *nrf2*^{+/+} mice but not *nrf2*^{-/-} mice. An aqueous broccoli seed extract was prepared for treatment of cultured cells that contained ITC at ~600 μ mol/L, composed of 61% 3-methylsulfinyl-propyl ITC, 30% sulforaphane, 4% allyl ITC, and 4% 3-butenyl ITC. This extract induced GSTA1/2, GSTA3, NQO1; and GCLC between 3-fold and 10-fold in mouse Hepa-1c1c7 and rat liver RL-34 cells. The broccoli seed extract affected increases in GSTA3, GSTM1, and NQO1 proteins in *nrf2*^{+/+} mouse embryonic fibroblasts but not in *nrf2*^{-/-} mouse embryonic fibroblasts. These experiments show that broccoli seeds are effective at inducing antioxidant and detoxication proteins, both in vivo and ex vivo, in an Nrf2-dependent manner. *J. Nutr.* 134: 3499S–3506S, 2004.

KEY WORDS: • antioxidant response element • chemoprevention • glucosinolates • sulforaphane • myrosinase

Individuals who have a high dietary intake of fruit and vegetables appear to have a lower risk of cancer (1). Among vegetables with anticarcinogenic properties, members of the Cruciferae family have been reported to protect against neo-

plastic disease at a variety of sites, such as the gastrointestinal tract and the lungs (2–6).

The cancer chemopreventive effect of cruciferous vegetables has been attributed to the fact that they contain high levels of glucosinolates (7,8). During food preparation and eating, these glucosinolates are hydrolyzed by the plant enzyme myrosinase to yield a complex number of breakdown products, including isothiocyanates (ITC),⁴ thiocyanates, cyanides, nitriles, and epithio-containing compounds (7–9).

¹ Published in a supplement to *The Journal of Nutrition*. Presented as part of the International Research Conference on Food, Nutrition, and Cancer held in Washington, DC, July 15–16, 2004. This conference was organized by the American Institute for Cancer Research and the World Cancer Research Fund International and sponsored by BASF Aktiengesellschaft; Campbell Soup Company; The Cranberry Institute; Danisco USA Inc.; DSM Nutritional Products, Inc.; Hill's Pet Nutrition, Inc.; Kellogg Company; National Fisheries Institute; The Solae Company; and United Soybean Board. An educational grant was provided by The Mushroom Council. Guest editors for this symposium were Helen A. Norman, Vay Liang W. Go, and Ritva R. Butrum.

² Supported by grant 2000/11 from the World Cancer Research Fund and by grant G0000268 from the Medical Research Council of the UK (L.G.H.).

³ To whom correspondence should be addressed.
E-mail: john.hayes@cancer.org.uk.

⁴ Abbreviations used: AITC, allyl isothiocyanate; ARE, antioxidant response element; GCLC, glutamate cysteine ligase catalytic; GCLM, glutamate cysteine ligase modifier; GST, glutathione S-transferase; ITC, isothiocyanate; LC-MS/MS, liquid chromatography with triple quadrupole mass spectrometric detection; MEF, mouse embryonic fibroblast; MRM, multiple reaction monitoring; NQO1, NAD(P)H:quinone oxidoreductase 1; Nrf2, nuclear factor-erythroid 2 p45-related factor 2.

Some of these breakdown products, and, in particular, ITCs can increase the levels of detoxication enzymes in rodent organs and in mouse, rat, and human cell lines (10–17). Inducible proteins include the drug-metabolizing enzymes aldo-keto reductase, NAD(P)H:quinone oxidoreductase 1 (NQO1), and glutathione S-transferase (GST). Increases in the levels of these detoxication enzymes would be expected to confer protection against chemical carcinogens such as benzo[a]pyrene, and, in experimental models, this prediction appears to hold true (14,18). Less well appreciated is the fact that glucosinolate breakdown products also induce antioxidant proteins, such as the glutamate cysteine ligase catalytic (GCLC) and glutamate cysteine ligase modifier (GCLM) subunits, that catalyze the rate-limiting step in the formation of reduced glutathione (19,20). They also induce glutathione reductase, ferritin, and glucose-6-phosphate dehydrogenase (20). Increases in the levels of detoxication enzymes and antioxidant proteins would be expected to protect against reactive oxygen species and the harmful metabolites they generate as a consequence of damaging cellular membranes, proteins, and nucleic acids (21).

Many genes encoding detoxication and antioxidant proteins are regulated by nuclear factor-erythroid 2 p45-related factor 2 (Nrf2) (22). This basic-region leucine zipper transcription factor mediates the transcriptional activation of genes in response to oxidative and electrophile stress. Under normal homeostatic conditions, Nrf2 protein has a short half-life, being targeted for proteasomal degradation by Keap1 (23–26). Oxidants and electrophiles interfere with Keap1-facilitated degradation of Nrf2, causing it to become more stable. This process involves oxidation, modification, or both, of cysteine residues 273 and 288 in Keap1 by the inducing compounds (27). Induction of NQO1, GST, GCLC, and GCLM genes by Nrf2 occurs through it being recruited to antioxidant response elements (ARE) in their gene promoters (28); Nrf2 binds the ARE as a heterodimer with small Maf proteins (29,30). Mice in which the *nrf2* gene has been disrupted by targeted homologous recombination have lower constitutive levels of NQO1 and GST proteins in liver and small intestine (19,31,32). Furthermore, *nrf2*^{-/-} mice are either unable to respond or have a blunted response to the model cancer chemopreventive agent butylated hydroxyanisole (19,33,34).

Most investigations into the ability of plant chemicals to increase antioxidant gene expression used highly purified compounds as inducing agents (11–20). Thus, ITCs such as sulforaphane have been shown to increase NQO1 enzyme activity in the mouse liver Hepa-1c1c7 cell line (35). Frequently, it is unclear whether the concentration of phytochemical used in cell culture experiments is physiologically relevant and whether, because of limitations caused by bioavailability or disposition, the dose of chemical used can be achieved in target tissues *in vivo*. The question of whether extracts of cruciferous plants are as effective as purified phytochemicals at stimulating gene expression is seldom addressed.

In this study, we investigated whether broccoli seeds, either in the diet or as aqueous extracts, can affect induction of antioxidant and detoxication genes *in vivo*, in transformed cells, and in nontransformed cells. We also tested the hypothesis that Nrf2, through stimulating ARE-driven gene transcription, is essential for gene induction by broccoli-derived phytochemicals.

MATERIALS AND METHODS

Chemicals

Allyl ITC (AITC) and sulforaphane were obtained from Aldrich and LKT Laboratories, respectively. All other chemicals used were of the highest purity that was available from commercial suppliers.

Broccoli seeds

Broccoli seeds were purchased from Thompson and Morgan.

Processing of broccoli seeds for induction experiments

The broccoli seeds were processed at room temperature (20°C). Extracts were prepared by crushing 10 g seeds (dry weight), by pestle and mortar, to a fine powder. For mice feeding experiments, crushed broccoli seeds were added directly to powdered RM1 laboratory animal feed (SDS) at 15% by weight. For cell culture experiments, the broccoli seed powder was suspended in 3 volumes of distilled water and was mixed vigorously for 5 min. The suspension was centrifuged at 800 × *g* for 10 min before being filtered through a 0.2- μ m sterile filter. Aliquots (1 mL) of the aqueous filtered extract were snap-frozen in liquid nitrogen and were stored at -70°C before use; the entire process from crushing the broccoli seeds to snap-freezing the filtered aqueous extract was completed within 30 min. The frozen extracts were thawed rapidly and diluted 1/1000 in 6 mL of medium for cell culture experiments that were conducted in 60-mm dishes.

Analysis of glucosinolates and ITCs in broccoli seeds

Glucosinolates and corresponding ITCs were identified by liquid chromatography with triple quadrupole MS detection (LC-MS/MS). Standard reference glucosinolates were isolated and purified from *Brassica* seeds by modification of published methods (36), and the related ITCs were prepared by myrosinase-catalyzed hydrolysis (37) and purified by preparative reversed-phase HPLC. The following glucosinolates were analyzed by LC-MS/MS: sinigrin, gluconapin, progoitrin, glucoiberin, glucoraphanin, glucoalyssin, and gluconasturtiin and their related ITCs—AITC, 3-butenyl ITC, 5-vinyloxazolidine-2-thione, 3-methylsulfinylpropyl ITC, sulforaphane, 5-methylsulfinylpentyl ITC, and phenethyl ITC, respectively.

Glucosinolates and ITCs were determined in broccoli seeds by initial heating at 110°C for 2 h (to inactivate myrosinase). The seeds were then ground to a fine powder, lipid was removed by extraction with chloroform, and the residual solid was extracted twice with 75% methanol at 75°C. The combined methanol extracts were concentrated by removal of solvent under reduced pressure, filtered (0.2 μ m), spiked with authentic standard analytes, and analyzed by LC-MS/MS. For detection of ITCs in samples of seed extract and in culture medium, ITCs were extracted into dichloromethane and derivatized with ammonia (1.33 mol/L, 24 h at 20°C). The derivatized extracts were then evaporated under reduced pressure, reconstituted in 50% methanol, filtered (0.2 μ m), spiked with authentic standard analytes, and analyzed by LC-MS/MS.

Glucosinolates were detected by negative ion electrospray multiple reaction monitoring (MRM), where the fragment ion was hydrogen sulfate (38). Derivatized ITCs were detected by positive ion electrospray MRM, where fragmentation involved loss of ammonia. For LC-MS/MS, the HPLC column was a 100 × 2.1-mm octadecyl silica Symmetry column with a 10 × 2.1-mm guard column (Waters). The flow rate was 0.2 mL/min. The eluent was 0.1% (v:v) trifluoroacetic acid in water, with linear gradients of methanol (0–10% for glucosinolates and 0–80% for ITCs) over 30 min. Source and desolvation temperatures were 120 and 350°C, and the gas flows for cone and desolvation were 150 and 550 L/h, respectively. The capillary voltage was 2.50 kV, and the cone voltage was set at 50 V. Argon gas pressure in the collision cell was 2.9 × 10⁻³ mbar. Programmed molecular ions, fragment ions, and collision energies were optimized to ±0.1 Da and ±1 eV for MRM detection. Glucosinolate and ITC analytes were quantified by standard addition analysis. Samples ana-

lyzed were spiked with 1–100 pmol glucosinolate and 2–100 pmol ITC. The limits of detection for glucosinolates were ≤ 0.4 pmol and, for ITCs, were ≤ 2 pmol. The interbatch coefficients of variation were $< 5\%$, and recoveries were 80–100%.

Mice feeding experiments

The Ethical Review Committee of the University of Dundee approved this program of work, and, throughout the study, mice were treated as advised by regulations contained in the Animals and Scientific Procedure Act (1986) of the United Kingdom. The *nrf2*^{+/+} and *nrf2*^{-/-} mice were obtained as described previously (33). The mice used in this study have been backcrossed over 6 generations onto a C57BL/6 genetic background. Female mice of between 9 and 14 wk of age were used in all studies. Mice were fed on standard RM1 laboratory feed. Mice were given free access to RM1 feed with broccoli seeds at 15% (by weight) for 7 d immediately before being killed. During the administration of crushed broccoli seed, mice were monitored daily by measurement of body weight. Once the period of feeding these phytochemicals was complete, the mice were killed by exposure to a rising concentration of CO₂. Organs were removed and snap-frozen immediately in liquid nitrogen before being stored at -70°C .

Cell culture

Mouse Hepa-1c1c7 cells (European Collection of Animal Cell Cultures) were maintained in minimal essential Eagle's medium, with the Alpha modification (Sigma) supplemented with 10% (v:v) heat-inactivated fetal bovine serum, 50 U/mL penicillin-streptomycin mixture, and L-glutamine at 2 mmol/L. Rat liver RL-34 cells [Japanese Cancer Research Resources Bank (Setagaya-ku)] were grown in Dulbecco's modified Eagle's medium (Life Technologies) supplemented as described above. Wild-type and *Nrf2*-null mouse embryonic fibroblasts (MEF) were prepared from *nrf2*^{+/+} and *nrf2*^{-/-} mouse lines as described by Tiemann and Deppert (39). These cells were maintained in tissue culture flasks coated with 0.1% (w:v) gelatin for 30 min before use and were grown in medium supplemented with 10 $\mu\text{g/L}$ human recombinant epidermal growth factor, 1 \times insulin-transferrin-selenium (Gibco), and 10% (v:v) fetal bovine serum. All cell lines were maintained at 37°C and 5% CO₂.

The RL-34, Hepa-1c1c7, and MEF cells were cultured in monolayers and were allowed to grow to 80% confluence in 60-mm dishes before exposure for 24 h to phytochemicals. AITC and sulforaphane were both used to treat cells at a dose of 5 $\mu\text{mol/L}$. The aqueous broccoli seed extract used to treat cells contained several ITCs, with the total level in the culture media amounting to 0.6 $\mu\text{mol/L}$.

Enzyme assays and Western blotting

NQO1 enzyme activity was estimated by measuring the dicoumarol-inhibitable fraction of dichlorophenol indophenol reductase activity. GST enzyme activity was measured using 1-chloro-2,4-dinitrobenzene. Western blotting using antibodies against NQO1; class Alpha, Mu, and Pi GST isoenzymes; and GCLC subunits was conducted as reported previously (12,19,31).

DNA transfection and luciferase reporter gene assays

Transfection and ARE-reporter gene assays were performed in Hepa-1c1c7 cells. The wild-type mouse *nqo1* promoter reporter construct, containing the functional ARE (5'-TCACAGTGAGTCG-GCAAAATT-3') in the pGL3-Basic luciferase reporter vector, was described previously and was designated -1016/*nqo5'*-luc (29). The mutant NQO1 reporter construct containing 1016 nucleotides of 5'-upstream *nqo1* sequence but with the ARE scrambled (i.e., 5'-TTAGAGATACTAGACCACGTC-3', with mutated bases in italics) is called Mut1 (29). Transfection of -1016/*nqo5'*-luc and Mut1 into Hepa-1c1c7 cells was performed using Lipofectin Reagent (Life Technologies), and, in all experiments, the pRL-TK *Renilla* reporter vector (Promega) was used as an internal control. *Renilla* and firefly

luciferase activities were measured using the Dual-Luciferase Reporter Assay System (Promega).

RESULTS

Glucosinolates present in broccoli seeds

The glucosinolate content of broccoli seeds was examined before their ability to induce gene expression in mammalian cells was examined. Prior heating, to inactivate myrosinase, followed by LC-MS/MS analysis revealed that the seeds contained 38.8 mmol glucosinolates per kg. Glucoiberin accounted for 59% of the total glucosinolate recovered, whereas sinigrin and glucoraphanin accounted for 19 and 8% of the glucosinolates, respectively. Significant amounts of progoitrin, gluconapin, and gluconasturtiin were also detected (Table 1). The structures of these phytochemicals are shown in Figure 1.

Broccoli seeds induce NQO1 and GST in *nrf2*^{+/+} but not in *nrf2*^{-/-} mice

Feeding *nrf2*^{+/+} mice diets containing 15% (w:w) crushed broccoli seeds resulted in the induction of both NQO1 and GST enzyme activities in the stomach, the small intestine, and the liver, but no increase was observed in the large intestine.

In the wild-type mice, feeding the seeds increased NQO1 activity in the stomach from 155 ± 40 to 248 ± 50 nmol \cdot min⁻¹ \cdot mg⁻¹ protein; in the small intestine, the broccoli seed diet increased NQO1 activity from 106 ± 16 to 183 ± 8 nmol \cdot min⁻¹ \cdot mg⁻¹ protein; and, in the liver, this diet increased NQO1 activity from 50 ± 7 to 72 ± 4 nmol \cdot min⁻¹ \cdot mg⁻¹ protein. The NQO1 enzyme activity in the stomach, the small intestine, and the liver of *nrf2*^{-/-} mice placed on a control diet was only 50 ± 16 , 40 ± 20 , and 7 ± 5 nmol \cdot min⁻¹ \cdot mg⁻¹ protein, respectively. The NQO1 enzyme activity did not appear to be increased in stomach, the small intestine, or the liver of *nrf2*^{-/-} mice fed diet containing broccoli seeds.

In *nrf2*^{+/+} mice, feeding the broccoli seed diet for 7 d increased GST activity in the stomach from 1.55 ± 0.10 to 2.53 ± 0.47 $\mu\text{mol} \cdot \text{min}^{-1} \cdot \text{mg}^{-1}$ protein, in the small intestine from 1.61 ± 0.11 to 2.02 ± 0.23 $\mu\text{mol} \cdot \text{min}^{-1} \cdot \text{mg}^{-1}$ protein, and in the liver from 4.91 ± 0.52 to 7.7 ± 0.95 $\mu\text{mol} \cdot \text{min}^{-1} \cdot \text{mg}^{-1}$ protein. Not only was transferase activity substantially lower in *nrf2*^{-/-} mice than in the wild-type mice, but also, it was not increased in the mutant mice fed broccoli seeds. In stomach, small intestine, and liver, GST activity in knockout mice on a control diet was 1.26 ± 0.11 , 1.18 ± 0.12 , and 1.72 ± 0.69 $\mu\text{mol} \cdot \text{min}^{-1} \cdot \text{mg}^{-1}$ protein, respectively.

The levels of NQO1 protein in the tissues of mice fed

TABLE 1

Glucosinolate content of broccoli seeds

| Glucosinolate | Amount | % |
|-----------------|----------------|----|
| | mmol/kg | |
| Sinigrin | 7.5 \pm 1.0 | 19 |
| Gluconapin | 1.3 \pm 0.2 | 3 |
| Progoitrin | 2.7 \pm 0.4 | 7 |
| Glucoiberin | 23.2 \pm 3.6 | 59 |
| Glucoraphanin | 3.2 \pm 0.4 | 8 |
| Glucoalyssin | 0.2 \pm 0.04 | 1 |
| Gluconasturtiin | 0.9 \pm 0.3 | 2 |

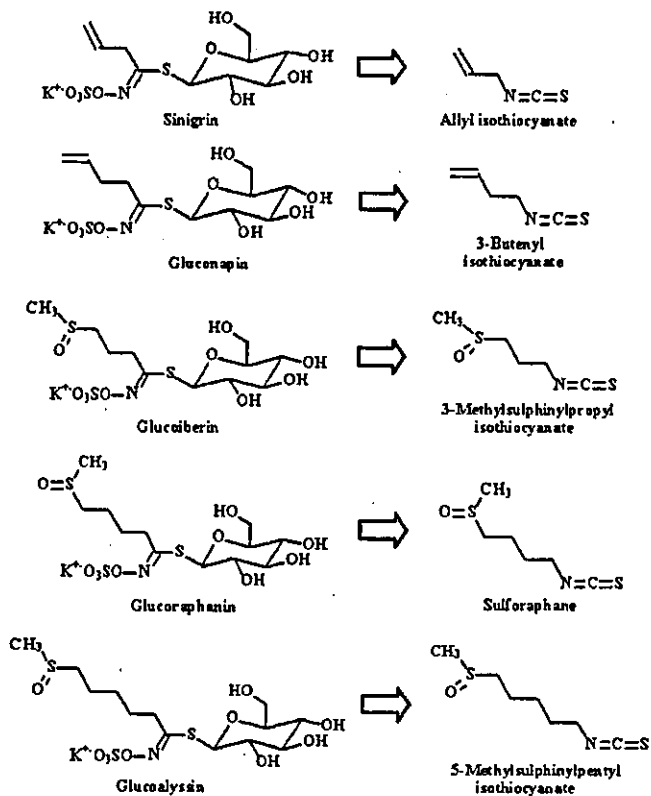


FIGURE 1 Glucosinolates (left) and ITCs (right) obtained from broccoli seeds.

broccoli seeds was examined by Western blotting to determine whether increases in oxidoreductase activity in stomach, small intestine, and liver reflected an increase in protein. Immunoblotting showed increases of ~2-fold in the level of NQO1 in all 3 organs from *nrf2*^{+/+} mice administered broccoli seeds (Figs. 2 and 3). Similar experiments were carried out using antisera against class Alpha, Mu, and Pi GST subunits. These revealed significant increases of class Alpha GSTA3 protein in stomach and small intestine and a modest increase in all organs of class Mu GSTM1. The level of the class Pi GSTP1 subunit did not appear to increase in mice after administration of broccoli seeds.

Western blots showed a 5-fold increase in the level of GCLC in the stomach of *nrf2*^{+/+} mice fed broccoli seeds, and a more modest increase was also observed in the small intestine of wild-type mice (Fig. 2). By contrast, no increase was observed in the liver (Fig. 3). A decrease in GCLC protein levels was seen in the stomach, the small intestine, and the liver of *nrf2*^{-/-} mice compared with the same organs from wild-type mice. Furthermore, the protein was not induced in either stomach or small intestine of mutant mice fed broccoli seeds (Fig. 2).

Glucosinolate breakdown products identified in broccoli seed extracts

The total amount of glucosinolate in the broccoli seed extract was <3.6 $\mu\text{mol/L}$, whereas the total amount of ITC in the extract was 596 $\mu\text{mol/L}$. Table 2 shows that 3-methylsulfinylpropyl ITC and sulforaphane account for 61 and 30%,

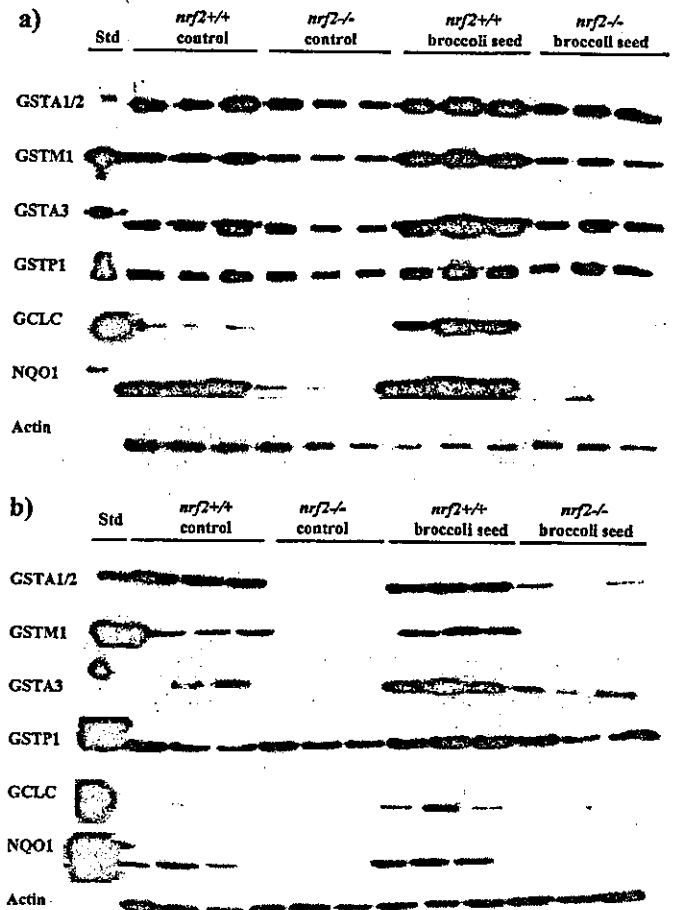


FIGURE 2 *Nrf2*-dependent induction of NQO1, GST, and GCLC proteins in stomach of mice fed broccoli seeds. Western blotting was performed on tissue extracts. Immunoreactive standards were applied to lane 1. Portions (10 μg protein) from stomach (panel a) or small intestine (panel b) of *nrf2*^{+/+} and *nrf2*^{-/-} mice fed on the RM1 control diet and from mice fed on RM1 diet containing 15% (w:w) crushed broccoli seeds were applied to the remaining lanes. Samples of tissue cytosol from 3 mice were applied to the gel.

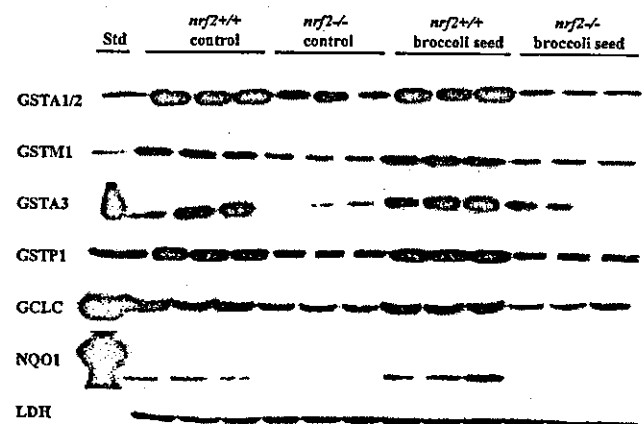


FIGURE 3 Induction of hepatic NQO1 and GST by broccoli seeds. Immunoblotting was performed on hepatic cytosol from wild-type and mutant mice as described. Lactate dehydrogenase (LDH) was used as a loading control for the samples.

TABLE 2

Isothiocyanates in broccoli seed extracts

| Parent glucosinolate | Isothiocyanate | Amount of isothiocyanate ¹ | |
|----------------------|-----------------------------|---------------------------------------|------|
| | | $\mu\text{mol/L}$ | % |
| Sinigrin | Allyl ITC | 25.0 | 4.2 |
| Gluconapin | 3-Butenyl ITC | 23.0 | 3.8 |
| Progoitrin | 5-Vinyloxazolidine-2-thione | nd | — |
| Glucoiberin | 3-Methylsulfinylpropyl ITC | 364.0 | 61.1 |
| Glucoaphanin | Sulforaphane | 177.0 | 30.0 |
| Glucoalyssin | 5-Methylsulfinylpentyl ITC | 5.5 | 0.9 |
| Gluconasturtiin | Phenethyl ITC | 1.2 | 0.2 |

¹ nd, not determined.

respectively, of the ITCs present in the seed extract. Significant amounts of AITC and 3-butenyl ITC were also obtained.

Induction of NQO1 and GST in rodent liver cell lines by broccoli-derived chemicals

Aqueous broccoli seed extracts were used to treat cells at an estimated concentration of total ITC of 0.6 $\mu\text{mol/L}$ in the media. The transformed mouse Hepa-1c1c7 liver cell line and the nontransformed rat liver RL-34 epithelial cells were used in these experiments. The broccoli seed extract increased NQO1 enzyme activity ~ 3 -fold and ~ 5 -fold in the Hepa-1c1c7 and RL-34 cells, respectively. Treatment with AITC at 5 $\mu\text{mol/L}$ induced NQO1 catalytic activity ~ 2 -fold in both Hepa-1c1c7 and RL-34 cells. Treatment with sulforaphane at 5 $\mu\text{mol/L}$ induced NQO1 catalytic activity 4.5-fold and 5.2-fold in Hepa-1c1c7 and RL-34 cells, respectively. By contrast, GST activity was not increased to the same extent in either cell line.

Western blotting showed that the level of NQO1 protein in Hepa-1c1c7 and RL-34 cells (Fig. 4A and B, respectively) grown in normal cell culture medium without the addition of phytochemicals was barely detectable. Treatment of both cell lines with the broccoli seed extract containing a mixture of ITCs substantially increased NQO1 protein. This increase was comparable to the induction of NQO1 protein affected by sulforaphane at 5 $\mu\text{mol/L}$.

Immunoblots were carried out to determine whether the broccoli extracts induced the various GST subunits. The levels of the class Alpha GSTA1/2 and GSTA3 subunits were found to be increased by the broccoli extract, and the degree of induction was similar to that obtained using sulforaphane.

In both Hepa-1c1c7 and RL-34 cells, the broccoli seed extract induced large increases in GCLC protein (Fig. 4).

Broccoli seed extracts stimulate ARE-driven gene expression

To determine whether broccoli seed extracts can activate gene expression controlled through an ARE enhancer, RL-34 cells were transfected with the mouse $-1016/nqo5'$ -luc reporter construct. Treatment of transfected cells with the standard dose of broccoli seed extract produced a 4.6-fold increase in luciferase activity compared with transfected cells treated with vehicle alone (Fig. 5). By contrast, AITC and sulforaphane, each at 5 $\mu\text{mol/L}$, produced 1.9-fold and 3.3-fold

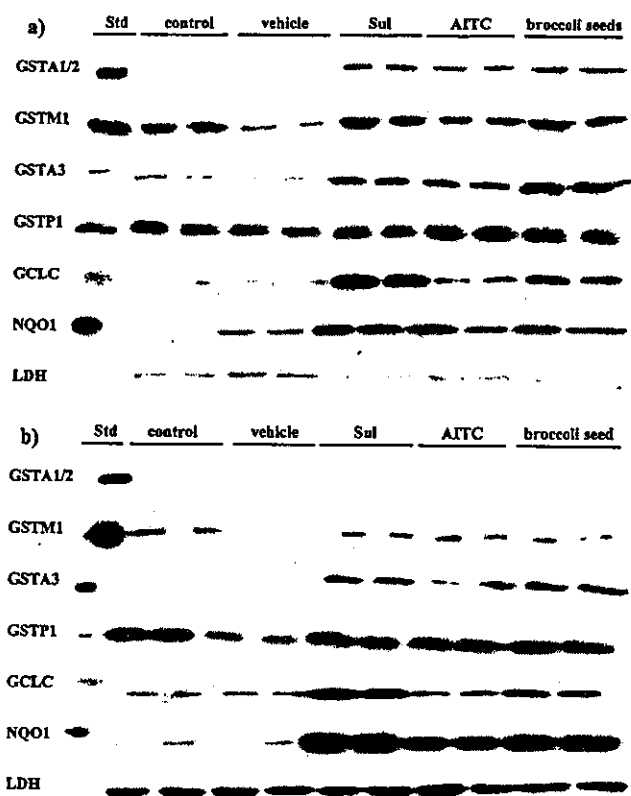


FIGURE 4 Induction of NQO1, GST, and GCLC by broccoli seed extracts in rodent liver cell lines. Cells were grown in either media alone or for 24 h in media containing sulforaphane (Sul; 5 $\mu\text{mol/L}$), AITC (5 $\mu\text{mol/L}$), or 1/1000 dilution of broccoli seed extract. Protein standards were applied to lane 1. The other samples are duplicates of individual treatments taken from separate flasks. Panel A shows data from the transformed Hepa-1c1c7 cells and panel B shows data from the non-transformed rat liver RL-34 cells.

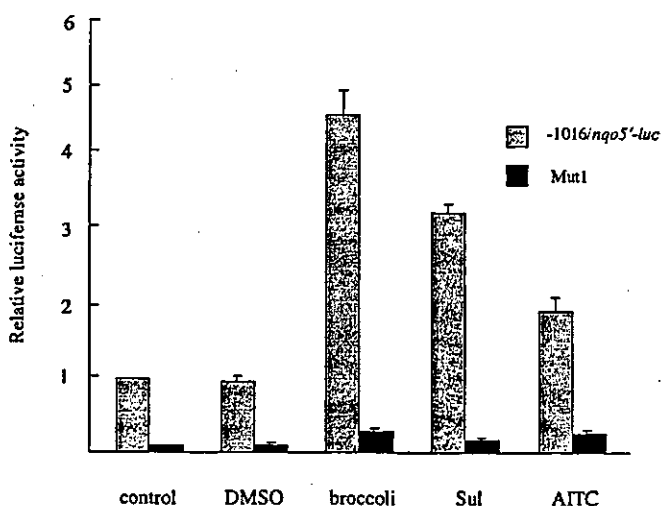


FIGURE 5 Broccoli seed extracts stimulate ARE-driven gene expression. Mouse Hepa-1c1c7 cells were transfected with a luciferase reporter construct driven by the wild-type mouse *nqo1* promoter ($-1016/nqo5'$ -luc) or by the same promoter containing a scrambled ARE (Mut1); pRL-TK *Renilla* reporter vector was used as an internal control. Sixteen hours after transfection, cells were treated for 24 h with 1/1000 dilution of broccoli seed extract, sulforaphane (Sul; 5 $\mu\text{mol/L}$), AITC (5 $\mu\text{mol/L}$), or dimethyl sulfoxide (0.1% v/v).

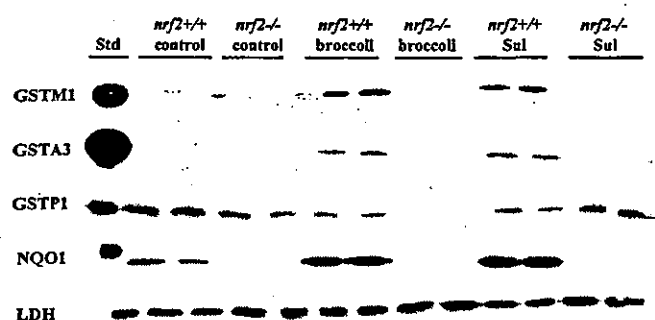


FIGURE 6 Nrf2-dependent induction of NQO1 and GST in mouse embryonic fibroblasts. Wild-type and Nrf2-null MEFs were derived and maintained as described. In the control treatment group the MEFs were grown in medium supplemented with epidermal growth factor, insulin-transferrin-selenium, and 10% fetal bovine serum. Treatment with broccoli seed extract involved growing MEFs in medium for 24 h with 1/1000 dilution of the filtered aqueous seed extract. The sulforaphane (Sul) treated MEFs were grown for 24 h in the presence of ITC (5 $\mu\text{mol/L}$).

increases, respectively, in luciferase activity. Similar experiments using a reporter construct driven by the mouse *nqo1* promoter that contained a mutant ARE (i.e., Mut1) proved to be unresponsive to broccoli seed extract, AITC, and sulforaphane.

Induction of GST and NQO1 by broccoli seed extracts is abolished in *nrf2*^{-/-} mouse embryonic fibroblasts

To explore whether GST subunits and NQO1 can be induced by broccoli in an Nrf2-dependent fashion, wild-type and mutant MEFs were treated with the seed extract. In the *nrf2*^{+/+} MEFs, treatment with the standard dose of broccoli seed extract caused a significant increase in GSTM1, GSTA3, and NQO1. This increase was similar to that seen in wild-type MEFs treated with sulforaphane at 5 $\mu\text{mol/L}$. In the *nrf2*^{-/-} MEFs, the levels of GSTM1, GSTA3, and NQO1 were lower than in the wild-type cells, and the seed extract failed to induce these proteins (Fig. 6).

DISCUSSION

An increasing body of evidence suggests that high intake of cruciferous vegetables can protect against tumorigenesis (2–6). One mechanism proposed to explain this conclusion is that glucosinolates, which are uniquely abundant in these plants, are converted by the actions of myrosinase to thiol-active metabolites that can stimulate cytoprotective responses in cells of the host (40). The major group of phytochemicals that are believed to stimulate such defenses are ITCs, and these compounds can induce the expression of ARE-driven genes. An alternative hypothesis is that ITCs can cause arrest at the G2/M phase of the cell cycle. This is associated with decreases in cyclin B1, Cdc25B, and Cdc25C proteins (41).

Most of the studies into the cellular effects of glucosinolate-derived compounds have used purified phytochemicals such as sulforaphane, benzyl ITC, and phenethyl ITC (2,14–18). How relevant the doses of pure phytochemical used in such gene induction and cell cycle arrest experiments are to the *in vivo* situation is unclear. This issue is complicated, because the yield of ITCs from different pa-

rental glucosinolates varies substantially and can be influenced significantly by the presence of epithiospecifier protein present in certain crucifers (9,42). In the present paper, broccoli seeds were used as the source of plant glucosinolates because we wished to avoid variations in the content of these chemicals that arise from postgermination metabolism. Furthermore, Fahey et al. (43) reported that the ability of broccoli to induce NQO1 in Hepa-1c1c7 cells diminishes with the age of the plant. Therefore, in this study, we used crushed broccoli seeds in the mice feeding experiments and aqueous seed extracts in the cell culture experiments. Analysis of the glucosinolates revealed that the seeds used in this study contained primarily glucoiberin and sinigrin, with lesser amounts of glucoraphanin and progoitrin (Table 1). In the aqueous broccoli seed extracts, LC-MS/MS revealed the presence of large amounts of ITCs, primarily 3-methylsulfinylpropyl ITC, and sulforaphane (Table 2). The low recovery of AITC in the extracts is noteworthy given the large amount of sinigrin in the broccoli seeds.

Enzyme assay and Western blotting showed that addition of broccoli seeds at 15% (w:w) in the RM1 diet induced NQO1 about 2-fold in stomach, small intestine, and liver of wild-type mice. No induction was observed in the *nrf2*^{-/-} mice. Similar results were observed by treating the *nrf2*^{+/+} and *nrf2*^{-/-} mouse embryonic fibroblasts with broccoli seed extracts. Because the promoter of mouse *nqo1* contains a functional ARE that recruits Nrf2 after treatment with sulforaphane (29), it is highly likely that transcriptional activation of mouse *nqo1* caused by preparations of broccoli seed is a direct consequence of ITCs stimulating the basic-region leucine zipper protein to transactivate directly the oxidoreductase gene.

Among GSTs, modest increases of GSTM1 protein were observed in the stomach and the small intestine of wild-type but not of *nrf2*^{-/-} mice after feeding with broccoli seeds. This diet also produced significant increases of the GSTA3 subunit in the stomach and large increases in the small intestine of wild-type mice. However, no such increases were observed in mutant mice. In MEFs from the wild-type and knockout mice, the Nrf2 dependency of induction of GSTM1 and GSTA3 by broccoli was clearly observed. Both the GSTM1 and GSTA3 subunit genes have been reported to contain an ARE (30,44), and it is likely that Nrf2 mediates induction directly through this enhancer. Chromatin immunoprecipitation experiments are required to confirm this hypothesis.

In the stomach and the small intestine of wild-type mice, substantial increases in GCLC were observed after treatment with the broccoli seed preparations. It is likely that Nrf2 mediates the increase in mouse GCLC and requires the existence of a functional ARE in the gene promoter, because this occurs in the human gene (45). However, the presence of a functional ARE in mouse *gclc* remains to be established.

Cellular models for screening the cancer chemopreventive properties of phytochemicals have frequently used induction of NQO1 enzyme activity in Hepa-1c1c7 cells (46). Our study revealed that besides NQO1 induction, GSTA1/2, GSTA3, and GCLC are also increased significantly in this transformed cell line by broccoli seed extract and by sulforaphane. Importantly, we also found that in nontransformed RL-34 cells, the seed extract and sulforaphane cause large increases in NQO1 and GCLC proteins. Modest increases in GSTA3 were also observed. Nakamura et al. (13) suggested that measurement of GST activity in RL-34 cells provides a useful assay for identifying potential inducing agents. However, our data suggest that induction of NQO1 in these cells may provide the most

sensitive assay to identify chemopreventive phytochemicals, because the Western blots in Figure 4 suggest that a 10-fold increase of the protein can be readily achieved.

Significant variations in the amounts and the types of glucosinolates in different broccoli strains appear to exist (7–9). Because this will result in distinct ITCs being generated by myrosinase from different broccoli strains, these differences in glucosinolate content will also influence the level of induction that can be achieved in the host and also possibly the sensitivity to cell-cycle arrest. The significance of variation in the glucosinolate content of cruciferous vegetables in terms of antioxidant and detoxication gene induction and stimulation of cell-cycle arrest and apoptosis warrants further study.

ACKNOWLEDGMENT

We thank Jed Fahey for valuable constructive criticism of this work during the AICR conference and for pointing out the confounding effects of epithiospecifier protein on glucosinolate degradation.

LITERATURE CITED

- Block, G., Patterson, B. & Subar, A. (1992) Fruit, vegetables, and cancer prevention: a review of the epidemiological evidence. *Nutr. Cancer* 18: 1–29.
- Verhoeven, D.T.H., Verhagen, H., Goldbohm, R. A., van den Brandt, P. A. & van Poppel, G. (1997) A review of mechanisms underlying anticarcinogenicity by brassica vegetables. *Chem. Biol. Interact.* 103: 79–129.
- Van Poppel, G., Verhoeven, D. T., Verhagen, H. & Goldbohm, R. A. (1999) Brassica vegetables and cancer prevention. *Epidemiology and mechanisms. Adv. Exp. Med. Biol.* 472: 159–168.
- Steinkellner, H., Rabot, S., Freywald, C., Nobis, E., Scharf, G., Chabicovsky, M., Knasmüller, S. & Kassie, F. (2001) Effects of cruciferous vegetables and their constituents on drug metabolising enzymes involved in the bioactivation of DNA-reactive dietary carcinogens. *Mutat. Res.* 480–481: 285–297.
- Talalay, P. & Fahey, J. W. (2001) Phytochemicals from cruciferous plants protect against cancer by modulating carcinogen metabolism. *J. Nutr.* 131: 3027S–3033S.
- Conaway, C. C., Yang, Y.-M. & Chung, F.-L. (2002) Isothiocyanates as cancer chemopreventive agents: their biological activities and metabolism in rodents and humans. *Curr. Drug Metab.* 3: 233–255.
- Fenwick, G. R., Heaney, R. K. & Mullin, W. J. (1983) Glucosinolates and their breakdown products in food and food plants. *CRC Crit. Rev. Food Sci. Nutr.* 18: 123–201.
- Fahey, J. W., Zalcmann, A. T. & Talalay, P. (2001) The chemical diversity and distribution of glucosinolates and isothiocyanates among plants. *Phytochemistry* 56: 5–51.
- Matusheski, N. V., Juvik, J. A. & Jeffery, E. H. (2004) Heating decreases epithiospecifier protein activity and increases sulforaphane formation in broccoli. *Phytochemistry* 65: 1273–1281.
- Zhang, Y., Talalay, P., Cho, C. G. & Posner, G. H. (1992) A major inducer of anticarcinogenic protective enzymes from broccoli: isolation and elucidation of structure. *Proc. Natl. Acad. Sci. U.S.A.* 89: 2399–2403.
- Tawfiq, N., Heaney, R. K., Plumb, J. A., Fenwick, G. R., Musk, S.R.R. & Williamson, G. (1995) Dietary glucosinolates as blocking agents against carcinogenesis: glucosinolate breakdown products assessed by induction of quinone reductase activity in murine hepa1c1c7 cells. *Carcinogenesis* 16: 1191–1194.
- Kelly, V. P., Ellis, E. M., Manson, M. M., Chanas, S. A., Moffat, G. J., McLeod, R., Judah, D. J., Neal, G. E. & Hayes, J. D. (2000) Chemoprevention of aflatoxin B₁ hepatocarcinogenesis by coumarin, a natural benzopyrone that is a potent inducer of AFB₁-aldehyde reductase, the glutathione S-transferase A5 and P1 subunits, and NAD(P)H:quinone oxidoreductase in rat liver. *Cancer Res.* 60: 957–969.
- Nakamura, Y., Morimitsu, Y., Uzu, T., Ohigashi, H., Murakami, A., Naito, Y., Nakagawa, Y., Osawa, T. & Uchida, K. (2000) A glutathione S-transferase inducer from papaya: rapid screening, identification and structure-activity relationship of isothiocyanates. *Cancer Lett.* 157: 193–200.
- Bonnesen, C., Eggleston, I. M. & Hayes, J. D. (2001) Dietary indoles and isothiocyanates that are generated from cruciferous vegetables can both stimulate apoptosis and confer protection against DNA damage in human colon cell lines. *Cancer Res.* 61: 6120–6130.
- Brooks, J. D., Paton, V. G. & Vidanes, G. (2001) Potent induction of phase 2 enzymes in human prostate cells by sulforaphane. *Cancer Epidemiol. Biomark. Prev.* 10: 949–954.
- Morimitsu, Y., Nakagawa, Y., Haayashi, K., Fujii, H., Kumagai, T., Nakamura, Y., Osawa, T., Horio, F., Itoh, K., et al. (2002) A sulforaphane analogue that potently activates the Nrf2-dependent detoxification pathway. *J. Biol. Chem.* 277: 3456–3463.
- Jiang, Z.-Q., Chen, C., Yang, B., Hebbar, V. & Kong, A.-N.T. (2003) Differential responses from seven mammalian cell lines to the treatments of detoxifying enzyme inducers. *Life Sci.* 72: 2243–2253.
- Fahey, J. W., Haristoy, X., Dolan, P. M., Kensler, T. W., Scholtus, I., Stephenson, K. K., Talalay, P. & Lozniewski, A. (2002) Sulforaphane inhibits extracellular, intracellular, and antibiotic-resistant strains of *Helicobacter pylori* and prevents benzo[a]pyrene-induced stomach tumors. *Proc. Natl. Acad. Sci. U.S.A.* 99: 7610–7615.
- McMahon, M., Itoh, K., Yamamoto, M., Chanas, S. A., Henderson, C. J., McLellan, L. I., Wolf, C. R., Cavin, C. & Hayes, J. D. (2001) The cap'n'collar basic leucine zipper transcription factor Nrf2 (NF-E2 p45-related factor 2) controls both constitutive and inducible expression of intestinal detoxification and glutathione biosynthetic enzymes. *Cancer Res.* 61: 3299–3307.
- Thimmulappa, R. K., Mai, K. H., Srisuma, S., Kensler, T. W., Yamamoto, M. & Biswal, S. (2002) Identification of Nrf2-regulated genes induced by the chemopreventive agent sulforaphane by oligonucleotide microarray. *Cancer Res.* 62: 5196–5203.
- Hayes, J. D. & McLellan, L. I. (1999) Glutathione and glutathione-dependent enzymes represent a co-ordinately regulated defence against oxidative stress. *Free Rad. Res.* 31: 273–300.
- Motohashi, H., O'Connor, T., Katsuoka, F., Engel, J. D. & Yamamoto, M. (2002) Integration and diversity of the regulatory network composed of Maf and CNC families of transcription factors. *Gene* 294: 1–12.
- Nguyen, T., Sherratt, P. J., Huang, H. C., Yang, C. S. & Pickett, C. B. (2003) Increased protein stability as a mechanism that enhances Nrf2-mediated transcriptional activation of the antioxidant response element—degradation of Nrf2 by the 26 S proteasome. *J. Biol. Chem.* 278: 4536–4541.
- Itoh, K., Wakabayashi, N., Katoh, Y., Ishii, T., O'Connor, T. & Yamamoto, M. (2003) Keap1 regulates both cytoplasmic-nuclear shuttling and degradation of Nrf2 in response to electrophiles. *Genes Cells* 8: 379–391.
- McMahon, M., Itoh, K., Yamamoto, M. & Hayes, J. D. (2003) Keap1-dependent proteasomal degradation of transcription factor Nrf2 contributes to the negative regulation of antioxidant response element-driven gene expression. *J. Biol. Chem.* 278: 21592–21600.
- McMahon, M., Thomas, N., Itoh, K., Yamamoto, M. & Hayes, J. D. (2004) Redox-regulated turnover of Nrf2 is determined by at least two separate protein domains, the redox-sensitive Neh2 domain and the redox-insensitive Neh6 domain. *J. Biol. Chem.* 279: 31556–31567.
- Wakabayashi, N., Dinkova-Kostova, A. T., Holtzclaw, W. D., Kang, M. I., Kobayashi, A., Yamamoto, M., Kensler, T. W. & Talalay, P. (2004) Protection against electrophile and oxidant stress by induction of the phase 2 response: fate of cysteines of the Keap1 sensor modified by inducers. *Proc. Natl. Acad. Sci. U.S.A.* 101: 2040–2045.
- Nguyen, T., Sherratt, P. J. & Pickett, C. B. (2003) Regulatory mechanisms controlling gene expression mediated by the antioxidant response element. *Annu. Rev. Pharmacol. Toxicol.* 43: 233–260.
- Nioi, P., McMahon, M., Itoh, K., Yamamoto, M. & Hayes, J. D. (2003) Identification of a novel Nrf2-regulated antioxidant response element in the mouse NAD(P)H:quinone oxidoreductase 1 gene; reassessment of the ARE consensus sequence. *Biochem. J.* 374: 337–348.
- Jowsky, I. R., Jiang, Q., Itoh, K., Yamamoto, M. & Hayes, J. D. (2003) Expression of the aflatoxin B₁-8,9-epoxide-metabolizing murine glutathione S-transferase A3 subunit is regulated by the Nrf2 transcription factor through an antioxidant response element. *Mol. Pharmacol.* 64: 1018–1028.
- Hayes, J. D., Chanas, S. A., Henderson, C. J., McMahon, M., Sun, C., Moffat, G. J., Wolf, C. R. & Yamamoto, M. (2000) The Nrf2 transcription factor contributes both to the basal expression of glutathione S-transferases in mouse liver and to their induction by the chemopreventive synthetic antioxidants, butylated hydroxyanisole and ethoxyquin. *Biochem. Soc. Trans.* 28: 33–41.
- Nioi, P. & Hayes, J. D. (2004) Contribution of NAD(P)H:quinone oxidoreductase 1 to protection against carcinogenesis, and regulation of its gene by the Nrf2 basic-region leucine zipper and the Arylhydrocarbon receptor basic helix-loop-helix transcription factors. *Mutat. Res.* 555: 149–171.
- Itoh, K., Chiba, T., Takahashi, S., Ishii, T., Igarashi, K., Katoh, Y., Oyake, T., Hayashi, N., Satoh, K., et al. (1997) An Nrf2/small Maf heterodimer mediates the induction of phase II detoxifying enzyme genes through antioxidant response elements. *Biochem. Biophys. Res. Commun.* 236: 313–322.
- Chanas, S. A., Jiang, Q., McMahon, M., McWalter, G. K., McLellan, L. I., Elcombe, C. R., Henderson, C. J., Wolf, C. R., Moffat, G. J., et al. (2002) Loss of the Nrf2 transcription factor causes a marked reduction in constitutive and inducible expression of the glutathione S-transferase *Gsta1*, *Gsta2*, *Gstm1*, *Gstm2*, *Gstm3* and *Gstm4* genes in the livers of male and female mice. *Biochem. J.* 365: 405–416.
- Dinkova-Kostova, A. T., Fahey, J. W. & Talalay, P. (2004) Chemical structures of inducers of nicotinamide quinone oxidoreductase 1 (NQO1). *Methods Enzymol.* 382: 423–448.
- Barillari, J., Gueyerd, D., Rollin, P. & Iori, R. (2001) *Barbarea verna* as a source of 2-phenylethyl glucosinolate, precursor of cancer chemopreventive phenylethyl isothiocyanate. *Fitoterapia* 72: 760–764.
- Nastruzzi, C., Cortesi, R., Esposito, E., Menegatti, E., Leoni, O., Iori, R. & Palmieri, S. (2000) In vitro antiproliferative activity of isothiocyanates and nitriles generated by myrosinase-mediated hydrolysis of glucosinolates from seeds of cruciferous vegetables. *J. Agric. Food Chem.* 48: 3572–3575.
- Mellon, F. A., Bennett, R. N., Holst, B. & Williamson, G. (2002) intact glucosinolate analysis in plant extracts by programmed cone voltage electrospray

LC/MS: performance and comparison with LC/MS/MS methods. *Anal. Biochem.* 306: 83-91.

39. Tiemann, F. & Deppert, W. (1994) Immortalization of BALB/c mouse embryo fibroblasts alters SV40 large T-antigen interactions with the tumor suppressor p53 and results in a reduced SV40 transformation-efficiency. *Oncogene* 9: 1907-1915.
40. Dinkova-Kostova, A. T., Massiah, M. A., Bozak, R. E., Hicks, R. J. & Talalay, P. (2001) Potency of Michael reaction acceptors as inducers of enzymes that protect against carcinogenesis depends on their reactivity with sulfhydryl groups. *Proc. Natl. Acad. Sci. U.S.A.* 98: 3404-3409.
41. Singh, S. V., Herman-Antosiewicz, A., Singh, A. V., Lew, K. L., Srivastava, S. K., Kamath, R., Brown, K. D., Zhang, L. & Baskaran, R. (2004) Suiforaphane-induced G2/M phase cell cycle arrest involves checkpoint kinase 2-mediated phosphorylation of cell division cycle 25C. *J. Biol. Chem.* 279: 25813-25822.
42. Petroski, R. J. & Tookey, H. L. (1982) Interactions of thioglucoside glucosyltransferase and epithiospecifier protein of cruciferous plants to form 1-cyanoepithioalkanes. *Phytochemistry* 21: 1903-1905.
43. Fahey, J. W., Zhang, Y. & Talalay, P. (1997) Broccoli sprouts: an exceptionally rich source of inducers of enzymes that protect against chemical carcinogens. *Proc. Natl. Acad. Sci. U.S.A.* 94: 10367-10372.
44. Andorfer, J. H., Tchaikovskaya, T. & Listowsky, I. (2004) Selective expression of glutathione S-transferase genes in the murine gastrointestinal tract in response to dietary organosulfur compounds. *Carcinogenesis* 25: 359-367.
45. Wild, A. C., Moinova, H. R. & Mulcahy, R. T. (1999) Regulation of gamma-glutamylcysteine synthetase subunit gene expression by the transcription factor Nrf2. *J. Biol. Chem.* 274: 33627-33636.
46. Kang, Y. H. & Pezzuto, J. M. (2004) Induction of quinone reductase as a primary screen for natural product anticarcinogens. *Methods Enzymol.* 382: 380-414.



Original Contribution

Gene expression profiling of NRF2-mediated protection against oxidative injury

Hye-Youn Cho^{a,b,*}, Sekhar P. Reddy^a, Andrea DeBiase^c,
Masayuki Yamamoto^d, Steven R. Kleeberger^{a,b}

^aDepartment of Environmental Health Sciences, Johns Hopkins University Bloomberg School of Public Health, Baltimore, MD 21205, USA

^bLaboratory of Respiratory Biology, National Institute of Environmental Health Sciences,
National Institutes of Health, Research Triangle Park, NC 27709, USA

^cChildren's National Medical Center, George Washington University, Washington, DC 20010, USA

^dInstitute of Basic Medical Sciences and Center for Tsukuba, Advanced Research Alliance,
University of Tsukuba, Tennoudai, Tsukuba 305, Japan

Received 14 May 2004; accepted 6 October 2004

Available online 12 November 2004

Abstract

Nuclear factor E2 p45-related factor 2 (NRF2) contributes to cellular protection against oxidative insults and chemical carcinogens via transcriptional activation of antioxidant/detoxifying enzymes. To understand the molecular basis of NRF2-mediated protection against oxidative lung injury, pulmonary gene expression profiles were characterized in *Nrf2*-disrupted (*Nrf2*^{-/-}) and wild-type (*Nrf2*^{+/+}) mice exposed to hyperoxia or air. Genes expressed constitutively higher in *Nrf2*^{+/+} mice than in *Nrf2*^{-/-} mice included antioxidant defense enzyme and immune cell receptor genes. Higher basal expression of heat shock protein and structural genes was detected in *Nrf2*^{-/-} mice relative to *Nrf2*^{+/+} mice. Hyperoxia enhanced expression of 175 genes (\geq twofold) and decreased expression of 100 genes (\geq 50%) in wild-type mice. Hyperoxia-induced upregulation of many well-known/new antioxidant/defense genes (e.g., *Txnrd1*, *Ex*, *Cp-2*) and other novel genes (e.g., *Pkc- α* , *Tcf-3*, *Ppar- γ*) was markedly greater in *Nrf2*^{+/+} mice than in *Nrf2*^{-/-} mice. In contrast, induced expression of genes encoding extracellular matrix and cytoskeletal proteins was higher in *Nrf2*^{-/-} mice than in *Nrf2*^{+/+} mice. These NRF2-dependent gene products might have key roles in protection against hyperoxic lung injury. Results from our global gene expression profiles provide putative downstream molecular mechanisms of oxygen tissue toxicity.

© 2004 Elsevier Inc. All rights reserved.

Keywords: Microarray; Lung; Hyperoxia; Transcription factor; Antioxidant; Free radicals

Abbreviations: ANOVA, analysis of variance; AOX, aldehyde oxidase; ARE, antioxidant response element; CP, 1-Cys peroxiredoxin; DAB, 3,3'-diaminobenzidine tetrahydrochloride; EpRE, electrophilic response element; Ex, carboxylesterase; Gadd45, growth arrest and DNA damage-inducible 45 γ ; GGT, γ -glutamyl transpeptidase; G6PD, glucose-6-phosphate dehydrogenase; GPx, glutathione peroxidase; GSH, glutathione; GST, glutathione S-transferase; HO-1, heme oxygenase-1; HSP, heat shock protein; MAS5, Microarray Analysis Software 5; MMP, matrix metalloproteinase; NRF2, NF-E2 related factor 2; PKC, protein kinase C; PPAR γ , peroxisome proliferator-activated receptor γ ; pTyr, phosphorylated tyrosine; QTL, quantitative trait locus; ROS, reactive oxygen species; RT-PCR, reverse transcriptase-polymerase chain reaction; SOD, superoxide dismutase; TXNRD, thioredoxin reductase.

* Corresponding author. Fax: (410) 541 4133.

E-mail address: cho2@niehs.nih.gov (H.-Y. Cho).

Reactive oxygen species (ROS) have great potential to damage cellular proteins, lipids, and DNA and have been implicated in various diseases, including atherosclerosis, cancer, neurodegenerative disease, pulmonary fibrosis, and adult respiratory distress syndrome [1]. Oxidative stress results from an imbalance between excess production of ROS and limited cellular antioxidant defense capacity. Recent studies have expanded the known antioxidant defenses to include phase 2 detoxifying enzymes [e.g., NAD(P)H:quinone oxidoreductase 1 (NQO1), glutathione S-transferase (GST)], which have antioxidative roles through conversion and secretion of

harmful oxidized intermediates in malignant cells or tissues [2,3].

Inhalation exposure of laboratory animals to hyperoxia (>95% O₂) has been a useful model to investigate oxidative lung injury due to excess generation of ROS and severe pathology in airways [4,5]. The pathogenesis of oxygen-induced lung injury has been well characterized [6]. However, detailed molecular and mechanistic aspects are not completely understood. Hyperoxia increases expression or activity of many antioxidant enzymes in the lung [e.g., superoxide dismutase (SOD), glutathione peroxidase (GPx), catalase]. Several investigators have demonstrated important protective roles of these antioxidant enzymes in the pathogenesis of oxygen toxicity in laboratory rodents. For example, overexpression of pulmonary *Sod2* in mice provided partial protection against hyperoxic injury [7,8], and targeted deletion of *Sod2* enhanced susceptibility to oxygen [9]. It was also demonstrated that mice deficient in γ -glutamyl transpeptidase (GGT), one of the phase 2 enzymes involved in glutathione (GSH) recycling, had more diffuse lung injury and lower survival rate after hyperoxia exposure, compared to wild-type mice [10,11]. Another potent antioxidant, heme oxygenase-1 (HO-1, HSP32), was protective against oxygen injury in murine lung [12].

We previously identified a significant hyperoxia susceptibility quantitative trait locus (QTL) on chromosome 2 (hyperoxia susceptibility locus 1; *Hs11*) by genome-wide linkage analysis [13]. This QTL contained a candidate susceptibility gene, *Nrf2*, which encodes the transcription factor NF-E2-related factor 2 (NRF2). Recent investigations have established a critical role for NRF2 in combating oxidative stress generated by ROS, xenobiotics, chemical carcinogens, or other electrophiles in liver [14], lung [15,16], and various cells [17–19]. NRF2 transcriptionally induces antioxidant and defense enzyme genes by binding to the antioxidant response element (ARE) or electrophilic response element (EpRE) as a heterodimer with other transcription factors such as small Maf [15]. We determined that mice with targeted disruption of *Nrf2* had suppressed expression of several ARE-bearing antioxidant/detoxifying enzyme genes and their enzymatic activities after hyperoxia exposure, and these mice were significantly more susceptible to pulmonary oxygen toxicity, relative to wild-type mice [20].

The objective of this study was to identify lung gene expression profiles to understand the molecular mechanisms of oxygen toxicity and NRF2-mediated protection in murine lungs. Using mice with targeted disruption of *Nrf2* (*Nrf2*^{-/-}) and wild-type controls (*Nrf2*^{+/+}), we determined and compared comprehensive gene expression profiles of genes differentially regulated at baseline and in response to oxygen. Results of these studies identified novel pathways through which NRF2 may protect against oxidative tissue injury.

Experimental procedures

Animals

Breeding pairs of ICR/Sv129-*Nrf2*^{+/-} mice were obtained from a colony at Tsukuba University and maintained in the animal facility at the Johns Hopkins University Bloomberg School of Public Health. *Nrf2*^{+/+} and *Nrf2*^{-/-} mice were generated following the breeding procedures described previously [14]. Mice were fed a purified AIN-76A diet, and water was provided *ad libitum*. Cages were placed in laminar flow hoods with high-efficiency particulate-filtered air. Sentinel animals were examined periodically (titers and necropsy) for infection. All experimental protocols conducted in the mice were carried out in accordance with the standards established by the U.S. Animal Welfare Acts, set forth in NIH guidelines and the *Policy and Procedures Manual* (Johns Hopkins University Bloomberg School of Public Health Animal Care and Use Committee).

Oxygen exposure

Mice were placed on a fine mesh wire flooring in a sealed 45-l glass exposure chamber. Food and water were provided *ad libitum*. Sufficient humidified pure oxygen was delivered to the chamber to provide 10 changes/h (7 l/min flow rate). The concentration of oxygen in the exhaust from the chamber was monitored (Beckman OM-11, Irvine, CA, USA) throughout the experiments. The oxygen concentration for all experiments ranged from 95 to 99%. The chambers were opened once a day for <10 min to replace food and water. Male mice (6–8 weeks) of each genotype (*Nrf2*^{+/+}, *Nrf2*^{-/-}) were exposed to either room air or hyperoxia for 24, 48, and 72 h (*n* = 3/group).

Affymetrix GeneChip array analysis

Total RNA was isolated from the left lung of each mouse using Trizol reagent (Invitrogen, Gaithersburg, MD, USA). Double-stranded cDNA was synthesized from 6 μ g of total RNA using the SuperScript Choice system (Invitrogen) with an oligo(dT) primer containing a T7 RNA polymerase promoter (Genset, France). The isolated cDNA was purified by phenol/chloroform extraction and labeled using the ENZO BioArray RNA transcript labeling kit (Enzo Life Sciences, Inc., Farmingdale, NY, USA) to generate biotinylated cRNA. Biotin-labeled cRNA was purified with the Qiagen RNeasy kit (Qiagen, Inc., Valencia, CA, USA) and fragmented randomly to approximately 200 bp (200 mM Tris-acetate, pH 8.2, 500 mM KOAc, 150 mM MgOAc). Each fragmented cRNA sample was hybridized to an Affymetrix Murine Genome U74Av2 oligonucleotide array (Affymetrix, Inc., Santa Clara, CA, USA) for 16 h at 45°C in a GeneChip hybridization oven. Two array chips were used for pooled total RNA from

three mice per exposure group, per time point, per genotype. Microarrays were then washed and stained on the Affymetrix Fluidics Station 400 using instructions and reagents provided by Affymetrix. This involves removal of nonhybridized material and incubation with phycoerythrin–streptavidin to detect bound cRNA (scan 1). The signal intensity was amplified by second staining with biotin-labeled anti-streptavidin antibody, followed by phycoerythrin–streptavidin staining (scan 2). Fluorescent images were read using the Hewlett–Packard G2500A gene array scanner.

Analyses of array data

Each GeneChip underwent a stringent quality control regime. The following parameters were considered: cRNA fold changes (amount of cRNA obtained from starting RNA), scaling factor, percentage of “present” calls, signal intensity, housekeeping genes, internal probe set controls, and visual inspection of the data files for hybridization artifacts. The analysis was performed with Microarray Analysis Software 5 (MAS5) scaling to an average intensity of 800. The expression value (average difference) for each gene was determined by calculating the average of differences in intensity (perfect match intensity minus mismatch intensity) between its probe pairs. The expression analysis files created by MAS5 were transferred to GeneSpring 5.0 (Silicon Genetics, Redwood City, CA, USA) for statistical analyses and characterization of data. Mean intensity of each gene acquired from GeneChip replicates under eight experimental conditions was normalized to that in the air-exposed wild-type (*Nrf2*^{+/+}) group, and these relative ratios were used for all statistical comparison. Array data were analyzed in three ways. First, to determine the effect of NRF2 on basal gene expression, data from air-exposed (control) *Nrf2*^{+/+} and *Nrf2*^{-/-} mice were compared by Student's *t* test. Among significantly ($p < 0.01$) varied genes ($n = 383$), additional restriction identified genes that displayed more than twofold differences in their constitutive expression between genotypes. Second, data from wild-type animals (air, 24, 48, and 72 h) were analyzed by one-way analysis of variance (ANOVA) to determine genes significantly altered by hyperoxia exposure. A p value of 0.05 filtered out 446 genes. Genes increased or decreased more than twofold or 50%, respectively, over the air control at one or more time points were identified and further evaluated. Finally, to identify genes differentially regulated between *Nrf2*^{+/+} and *Nrf2*^{-/-} mice during hyperoxia exposure, data from all time points were first restricted by genotype, and then ANOVA filtered out 692 genes with p value of 0.05. Genotype-restricted genes were then further restricted by exposure to find genes ($n = 252$) significantly altered by hyperoxia ($p < 0.05$). The Benjamini and Hochberg False Discovery Rate test was used for the multiple comparisons as necessary. Gene tree applications clustered genes with similar expression pattern, and unique classes of genes with

similar kinetics were organized by *k*-means clustering. Gene ontology procedures were used to evaluate individual genes significantly altered by hyperoxia and significantly varied between *Nrf2*^{+/+} and *Nrf2*^{-/-} mice. Venn diagrams isolated common genes that varied basally and by hyperoxia between genotypes.

Total lung RNA isolation for reverse transcriptase-polymerase chain reaction (RT-PCR)

One microgram of total RNA was isolated from right lung homogenates in Trizol (Invitrogen) and was reverse transcribed into cDNA in a volume of 50 μ l. PCR amplifications were performed with aliquots of cDNA (5 μ l) using a specific primer set for each mouse gene as previously described [20]. Separate, simultaneous PCR for β -actin was done as an internal control, and the volume ratio of each gene cDNA band to β -actin cDNA band was determined using a Bio-Rad Gel Doc 2000 System (Hercules, CA, USA).

Protein isolation and Western blot analyses

Cytoplasmic and nuclear fractions were isolated from right lung homogenates of mice exposed to either air or hyperoxia (48, 72 h) using a Nuclear Extract Kit (Active Motif, Inc., Carlsbad, CA, USA) following the manufacturer's instructions. Cytoplasmic protein (50–100 μ g) was separated by sodium dodecyl sulfate–polyacrylamide gel electrophoresis, transferred to nitrocellulose membrane, and immunoblotted with specific primary antibodies for GST- α , GST- μ , and GPx2 (gifts from Dr. C.C. Reddy, Pennsylvania State University) or for glucose-6-phosphate dehydrogenase (G6PD; Novus Biologicals, Inc., Littleton, CO, USA), NQO1 (Novus Biochemicals), phosphorylated protein kinase C- α (*p*PKC- α ; Cell Signaling Technology, Inc., Beverly, MA, USA), phosphorylated tyrosine (*p*Tyr; Cell Signaling Technology), collagen type VI (Santa Cruz Biotechnology, Inc., Santa Cruz, CA, USA), HSP70 (Calbiochem Co., San Diego, CA, USA), laminin-B1 (NeoMarkers, Inc., Fremont, CA, USA), and vinculin (Upstate Group, Waltham, MA, USA). Krox-20 (Egr-2, Zfp-25) was detected in nuclear protein (50 μ g) using a specific antibody (Covance Research Products, Inc., Richmond, CA, USA). Western blotting was performed two to four times for each protein and representative band images of air and peak expression after hyperoxia are presented.

Lung tissue preparation for immunohistochemistry

Left lung tissues ($n = 2$ /group) excised from additional *Nrf2*^{+/+} or *Nrf2*^{-/-} mice exposed to hyperoxia (48 or 72 h) or air were inflated gently with zinc formalin, fixed under constant pressure for 30 min, and processed for paraffin embedding. Tissue sections (5 μ m thick) were immunologically stained using an affinity-purified rabbit polyclonal anti-

Table 1(A)
Representative genes expressed constitutively higher (\geq twofold) in *Nrf2*^{+/+} mice than in *Nrf2*^{-/-} mice

| Name | Accession No. | Description |
|---|---------------|--|
| Antioxidant enzymes and related | | |
| <i>Gstb-1</i> | J03952 | Glutathione S-transferase, μ 1 |
| <i>Gstb-2</i> | J04696 | Glutathione S-transferase, μ 2 |
| <i>Gstyc</i> | X65021 | Glutathione S-transferase, Yc |
| <i>Aox-1</i> | AB017482 | Retinal oxidase/aldehyde oxidase |
| <i>Nrf2</i> | U70475 | p45 NF-E2-related factor 2 |
| Cytochrome P450 hydroxylase | | |
| <i>Cyp15a1</i> | M19319 | Testosterone 15 α -hydroxylase, 2a4 |
| <i>Cyp2b</i> | M21856 | Testosterone phenobarbital inducible type b, 2b10 |
| G-protein-dependent signal transduction | | |
| <i>Gtp1</i> | AJ007972 | Interferon- γ -induced GTPase |
| <i>Grp-R</i> | RU84265 | G-protein-coupled, gastrin-releasing peptide receptor |
| <i>Grp1</i> | AF001871 | ARF1 guanine nucleotide exchange factor and integrin binding protein homolog |
| <i>Gpcr17</i> | D17292 | G protein-coupled receptor |
| Inflammation and immunity | | |
| <i>Cd3-ϵ</i> | M 23376 | CD3 antigen, ϵ polypeptide, T cell receptor complex |
| <i>Thy-1, Cd90</i> | M12379 | Thymus cell antigen 1, θ |
| <i>Nkg2d</i> | AF054819 | Natural killer costimulating receptor |
| <i>Tcra</i> | M16118 | T cell receptor α chain VJC precursor |
| <i>Lyl12</i> | U18424 | Bacterial binding macrophage receptor, MARCO |
| <i>Clqb</i> | M22531 | Complement component 1, q subcomponent, β polypeptide |
| <i>Lyl15</i> | AB023132 | Activation-inducible lymphocyte immunomediatory molecule (AILIM) |
| <i>Mip-1α receptor-like 1</i> | U28405 | MIP-1 α chemokine (C-C) receptor 1-like 1 |
| Others | | |
| <i>Tgf β1</i> | AJ009862 | Transforming growth factor- β 1 |
| <i>Ufo</i> | X63535 | AXL receptor tyrosine kinase |
| <i>Cftr11</i> | X72694 | Cystic fibrosis transmembrane conductance regulator |
| <i>P50, Pol1d2</i> | Z72486 | DNA polymerase δ small subunit |
| <i>Glut-3</i> | M75135 | Glucose transporter |
| <i>Pk-2, Pk-3</i> | X97047 | M2-type pyruvate kinase |
| <i>Epim</i> | D10475 | Epimorphin, morphogen |
| <i>Aq1</i> | L02914 | Aquaporin-1 |

NRF2 antibody raised against a peptide (16 amino acids) mapping at the C-terminus of mouse NRF2 (Covance Research Products, Inc.), an anti-GPx2 antibody, and an anti-collagen VI (α 1) antibody (Santa Cruz Biotechnology)

Table 1(B)
Representative genes expressed constitutively higher (\geq twofold) in *Nrf2*^{-/-} mice than in *Nrf2*^{+/+} mice

| Name | Accession No. | Description |
|---|---------------|---|
| Cell growth and maintenance | | |
| <i>Lop18</i> | J00376 | α -A-crystallin, small HSP homology |
| <i>Hsp68</i> | M12571 | 68 kDa heat shock protein |
| <i>Hsp-e71</i> | L40406 | Induced by HPV16E7 |
| <i>Cng</i> | L49507 | Cyclin G1 |
| <i>Mtiv</i> | U07808 | Metallothionein IV |
| <i>Fsp, Gro</i> | J04596 | Secretory protein KC precursor, GRO1 oncogene |
| Epidermal-related protein | | |
| <i>Krt-1.13</i> | X03492 | 47-kDa keratin |
| <i>Krt-2.4</i> | X03491 | 57-kDa keratin complex 2, basic |
| <i>Sprr2a</i> | AJ005559 | Small proline-rich protein 2A |
| <i>Sprr2b</i> | AJ005560 | Small proline-rich protein 2B |
| <i>Sprr3</i> | Y09227 | Small proline-rich protein 3 |
| <i>Lgals7</i> | AF038562 | Galectin-7, PIG-1, stratified epithelial cell marker |
| <i>Cx31</i> | X63099 | Connexin 31, keratinocyte epidermal connexin |
| Cytoplasm and extracellular matrix | | |
| <i>Myhs-p</i> | M12289 | Myosin, heavy polypeptide 8, skeletal muscle |
| Myosin light chain 2 | M91602 | Myosin light chain 2, putative |
| <i>Myhs-f</i> | AJ002522 | Myosin heavy chain 2 |
| Myosin alkali light chain | X12972 | Myosin alkali light chain |
| <i>Pgam2</i> | AF029843 | Phosphoglycerate mutase muscle-specific subunit |
| <i>Tnnt3</i> | L48989 | Troponin, skeletal muscle |
| <i>Fbn-1</i> | L29454 | Fibrillin |
| <i>Dy, Mer</i> | U12147 | Laminin-2 α 2 chain precursor |
| Others | | |
| <i>Slpi</i> | AF002719 | Secretory leukoprotease inhibitor |
| <i>Stk</i> | X74736 | Receptor tyrosine kinase |
| <i>Camkii</i> | X14836 | Calmodulin-dependent protein kinase II α |
| <i>Cox8h</i> | U15541 | Cytochrome c oxidase subunit VIII-H precursor |
| <i>Angrp</i> | U22519 | Angiogenin-related protein precursor |
| <i>Ada</i> | M14168 | Adenosine deaminase, conversion of adenosine to inosine |
| <i>Cacng1</i> | AJ006306 | Calcium channel, γ -subunit |

to localize NRF2, GPx2, and type VI collagen proteins, respectively, using a peroxidase–DAB method. GPx2-stained tissue sections were counterstained with hematoxylin.

Results

Constitutive mRNA expression in Nrf2^{+/+} and Nrf2^{-/-} mice

Three hundred eighty-three genes varied significantly ($p < 0.01$) between *Nrf2^{+/+}* and *Nrf2^{-/-}* mice at baseline. Genes ($n = 65$) that were expressed at least twofold more in *Nrf2^{+/+}* compared to *Nrf2^{-/-}* mice included those encoding NRF2, antioxidant/phase 2 enzymes, G-protein-linked signal transduction molecules, and T cell receptors (Table 1A). Genes ($n = 82$) that were expressed at least twofold higher in *Nrf2^{-/-}* compared to *Nrf2^{+/+}* mice included those encoding heat shock proteins, cytoskeleton/matrix components, and epidermal-related proteins (Table 1B).

Hyperoxia-altered gene expression profiles in Nrf2^{+/+} mice

We demonstrated previously that hyperoxia caused significant lung injury (i.e., inflammation and edema) 72 h after exposure in *Nrf2^{+/+}* mice; *Nrf2^{-/-}* mice were significantly more sensitive, with greater lung edema and inflammation after 48 and 72 h exposure compared to *Nrf2^{+/+}* mice [20]. Pulmonary *Nrf2* mRNA expression was increased immediately after hyperoxia exposure (1.5 h) and its nuclear DNA binding activity enhanced through 72 h in *Nrf2^{+/+}* mice [13,20]. Based on these findings, we determined time-dependent gene expression profiles before the onset of significant lung injury (24 h) and during the development of severe pathology (48 and 72 h). Hyperoxia significantly ($p < 0.05$) affected expression levels of 446 genes compared to air controls. Genes that were upregulated ($n = 218$) or downregulated ($n = 112$) at 24 h relative to air control levels remained elevated or suppressed, respectively, throughout the exposure (Fig. 1A). Six distinct patterns of gene expression were identified in the lungs of *Nrf2^{+/+}* mice during hyperoxia (Fig. 1B). Representative genes that were increased ($n = 175, \geq 2$ -fold) or decreased ($n = 100, \geq 50\%$) compared to each air control at least once during exposure are listed in Tables 2A and 2B. Sixty-six percent of the 446 genes were upregulated in a time-dependent manner by oxygen (Fig. 1B, sets 1, 2, 3, and 4). These include heat shock proteins, growth factor receptors/ligands, apoptosis proteins, signaling tyrosine phosphatases, extracellular matrix collagens and metalloproteinases, transcription factors/oncogenes, and various enzymes (Table 2A). Genes that were highly induced early (24 h) and remained elevated throughout the exposure included extracellular matrix and cytoskeletal genes (e.g., collagens, laminins, *Mmp-9*, *Vcl*, *Fbn-2*),

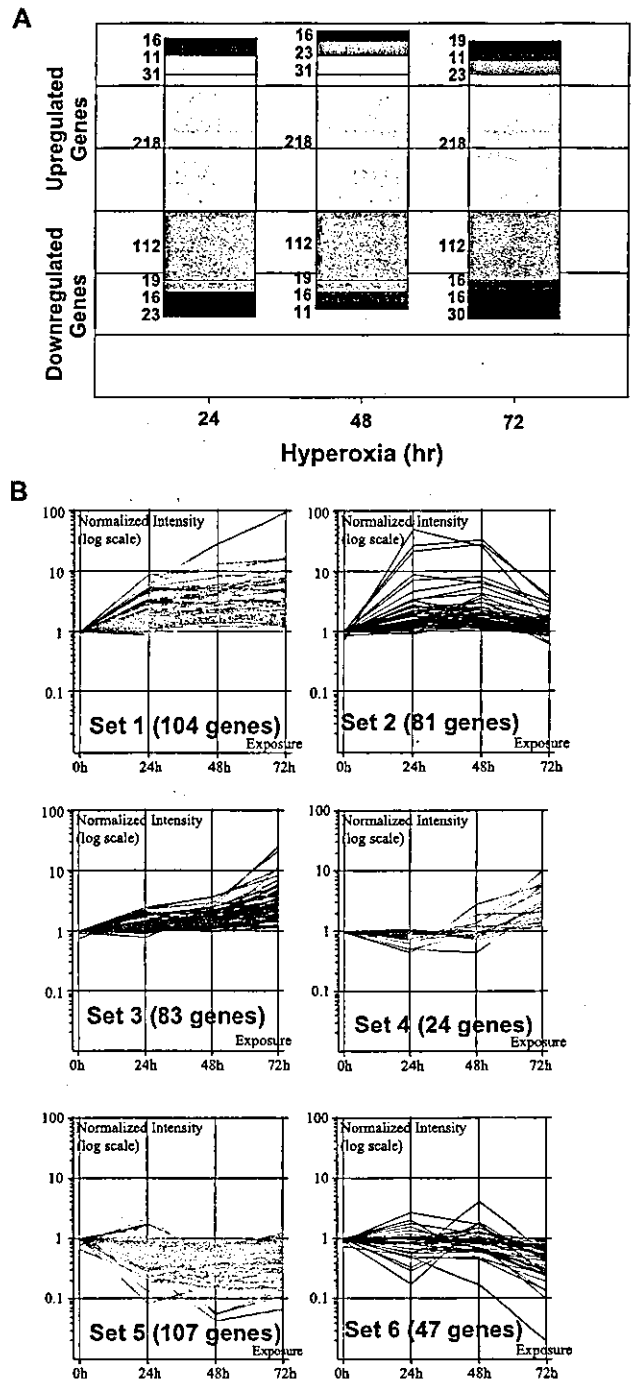


Fig. 1. (A) Number of genes significantly increased or decreased relative to air controls at each time of hyperoxia exposure in *Nrf2^{+/+}* mice. Matching colors of stacks indicate overlapping genes. (B) Six representative clusters of hyperoxia-induced (sets 1–4) and -suppressed (sets 5 and 6) genes classified based on expression patterns over time course (air and 24, 48, and 72 h O₂). Significantly altered genes ($n = 446, p < 0.05$) by hyperoxia in *Nrf2^{+/+}* mice were evaluated by *k*-means clustering analysis to determine association of gene expression kinetics with gene functions. Expression level of each time point of each gene was normalized by that of air control and expressed as relative log ratio.

inflammation-related genes (e.g., *Ly112*, *Cd104*, *Mic-1*, p-selectin ligand, *Et-1*, cytokine/chemokine/growth factor receptors), transcription factor genes and oncogenes (e.g.,

Table 2 (A)

Representative genes significantly increased (\geq twofold) by hyperoxia in the lungs of wild-type (*Nrf2*^{+/+}) mice

| Name | Accession No. | Description | Classification/function | Cluster subset (Fig. 1B) |
|--|---------------|---|--|--------------------------|
| Cell growth, death, and maintenance | | | | |
| <i>Hsp68</i> ^a | M12571 | 68-kDa Heat shock protein | Heat shock response | 3 |
| <i>Hsp40</i> | AB028272 | Heat shock protein 40 | Heat shock response | 3 |
| <i>Ho-1, Hsp32</i> | X56824 | Heme Oxygenase-1 | Heat shock response | 2 |
| <i>Nhe-1</i> | L40406 | Na ⁺ /H ⁺ exchanger | Cell pH and volume regulation | 1 |
| <i>Mic-1</i> ^a | AJ011967 | Macrophage inhibitory compound 1 | Growth factor ligand | 1 |
| <i>Activin</i> | X69620 | Inhibin β -B subunit, TGF receptor ligand | Growth factor ligand | 2 |
| <i>Fgfbp1</i> | AF06541 | Heparin/fibroblast growth factor binding protein 1 | Growth factor ligand | 2 |
| <i>Amphiregulin</i> ^a | L41352 | EGF family ligand | Growth factor ligand | 2 |
| <i>Acvr1k2</i> | L15436 | TGF- β type I receptor (Tsk 7L) | Growth factor receptor | 1 |
| <i>Mt-2</i> ^a | K02236 | Metallothionein II | Metal binding protein, antioxidant | 1 |
| <i>Cide-B</i> | AF041377 | Cell death activator | Apoptosis | 3 |
| Murine A20 | U19463 | A20 protein | Apoptosis | 4 |
| <i>Bax</i> | L22472 | Bax α | Apoptosis | 2 |
| <i>Gadd45</i> | U00937 | Growth arrest and DNA damage-inducible 45 γ | DNA repair, cell cycle check point control | 2 |
| Signal transduction | | | | |
| <i>Ptp36</i> | D31842 | Protein tyrosine phosphatase | Tyrosine phosphatase | 2 |
| <i>Ptprg</i> | L09562 | Protein tyrosine phosphatase, receptor type, GI | Tyrosine phosphatase | 1 |
| <i>Ntp1</i> ^a | X95518 | Neuronal tyrosine threonine phosphatase 1 | Tyrosine phosphatase | 1 |
| <i>Cd104</i> | L04678 | Integrin β 4 subunit | Integrin receptor signaling | 1 |
| <i>Calcr</i> | U18542 | Calcitonin receptor 1b, Ca ²⁺ -dependent | Calcium-dependent receptor signaling | 2 |
| <i>Mrp8</i> | M83218 | Intracellular calcium-binding protein | Calcium-dependent receptor signaling | 2 |
| <i>Rhoc</i> | X80638 | p21 Rho | Small GTP binding protein | 4 |
| <i>Ssecks</i> | AB020886 | Src suppressed C kinase substrate | Cytoskeletal signaling | 1 |
| Cellular components | | | | |
| <i>Coll1a1</i> | U03419 | Procollagen α 1 (I) | Extracellular matrix | 3 |
| <i>Col4a2</i> | X04647 | Collagen α 2 (IV) | Extracellular matrix | 1 |
| <i>Col6a1</i> | X66405 | Collagen α 1 (VI) | Extracellular matrix | 3 |
| <i>Mmp9</i> | X72795 | Gelatinase B | Extracellular matrix | 1 |
| <i>Mmp14</i> | AF022432 | Zinc endopeptidase | Extracellular matrix | 2 |
| <i>Vcl</i> | AI462105 | Vinculin cytoskeletal anchoring protein | Cytoskeleton | 1 |
| <i>Nf-66</i> ^b | L27220 | α internexin, neuronal intermediate filament protein | Cytoskeleton | 6 |
| <i>Laman</i> | U87240 | Lysosomal α mannosidase | Lysosome | 1 |
| <i>Gaa</i> | U49351 | Lysosomal α glucosidase | Lysosome | 3 |
| Cancer | | | | |
| <i>Fsp, Gro</i> | J04596 | Secretory protein KC precursor, GRO1 | Oncogene | 2 |
| <i>Rrg</i> | D10837 | Lysyl oxidase | Tumor suppressor | 1 |
| <i>Ufo</i> ^b | X63535 | AXL receptor tyrosine kinase | Oncogene | 6 |
| <i>Tx01</i> | Z31362 | Gene found in transformed mouse epidermal cell | Cancer related | 4 |
| <i>Meca39</i> | U42443 | Genetic target for c-Myc regulation | Cancer related | 1 |
| Transcription factors | | | | |
| <i>c-Fos</i> | V00727 | Fos cellular oncogene | Transcriptional activator | 2 |
| <i>Junc</i> | X12761 | Jun oncogene | Transcriptional activator | 1 |
| <i>Fra-1</i> ^a | AF017128 | Fos-related antigen 1 | Transcriptional activator | 2 |
| <i>Lrg-21</i> | U19118 | Leucine zipper protein | Transcriptional activator | 1 |
| <i>Hif1a</i> | AF003695 | Hypoxia-inducible factor 1 α | Transcriptional activator | 2 |
| <i>Sox6</i> ^a | AV246999 | EST, similar to Sox (sry-related gene) 6 | Transcriptional activator | 2 |
| Enzymes | | | | |
| <i>Pkc-α</i> | M25811 | Protein kinase C- α | Kinase | 1 |
| <i>Pkch</i> | D90242 | nPKC- η | Kinase | 2 |
| <i>Hkii</i> | Y11666 | Hexokinase II | Kinase | 1 |

Table 2 (A) (continued)

| Name | Accession No. | Description | Classification/function | Cluster subset (Fig. 1B) |
|----------------------------------|---------------|---|---------------------------------------|--------------------------|
| Enzymes | | | | |
| <i>Cyp15a1</i> | M19319 | Testosterone 15 α hydroxylase, 2a4 | Cytochrome P450 | 3 |
| <i>Cyp2b</i> | M21856 | Testosterone phenobarbital inducible type b, 2b10 | Cytochrome P450 | 1 |
| <i>Gcllc</i> | U85414 | γ -Glutamylcysteine synthetase | Glutathione biosynthesis enzyme | 2 |
| <i>Gfpr2</i> | AB016780 | Glutamine-fructose-6-phosphate amidotransferase 2 | Transferase | 1 |
| <i>Ggt</i> | U30509 | γ -Glutamyl transpeptidase, transmembrane | Transferase | 2 |
| <i>Pla2g7</i> | U34277 | PAF acetylhydrolase | Hydrolase | 2 |
| <i>Spi2/Eb4</i> | M64086 | Spi2 proteinase inhibitor | Proteinase inhibitor | 2 |
| <i>Mgk-3^b</i> | X00472 | γ -NGF, nerve growth factor, serine protease | Proteinase | 5 |
| <i>Mthfd2</i> | J04627 | NAD-dependent methylenetetrahydrofolate dehydrogenase | Hydrogenase | 2 |
| Inflammation and immunity | | | | |
| <i>Pai-1</i> | M33960 | Plasminogen activator inhibitor | | 2 |
| <i>Tpa</i> | J03520 | Tissue plasminogen activator precursor | Inflammatory peptide | 2 |
| <i>Il-6^b</i> | X54542 | Interleukin-6 precursor peptide | Cytokine | 4 |
| <i>Fic, Mcp3^a</i> | X70058 | Cytokine | Cytokine | 1 |
| <i>Socs-3</i> | U88328 | Suppressor of cytokine signaling-3 | Cytokine signaling negative regulator | 1 |
| <i>Il4r, Cd124</i> | M27960 | Interleukin 4 receptor, α | Cytokine receptor | 2 |
| <i>G-Csfr</i> | M58288 | Granulocyte colony-stimulating factor receptor | Cytokine receptor | 1 |
| <i>Ccr1, Mip-1a-r</i> | U29678 | MIP-1 α /Rantes receptor CCR-1 | Chemokine receptor | 1 |
| <i>V-1</i> | AJ132098 | Vanin 1 | Thymic antigen for leukocyte homing | 1 |
| <i>Ly112</i> | U18424 | Bacterial binding macrophage receptor, MARCO | Macrophage scavenger receptor | 1 |
| Others | | | | |
| <i>Et-1</i> | U35233 | Preproendothelin-1 | Vasoconstrictor | 1 |
| <i>Angl</i> | U72672 | Angiogenin-3 precursor | Angiogenesis | 3 |
| <i>Dii1</i> | X80903 | Delta-like 1 | Notch ligand | 1 |

^a Genes upregulated ≥ 10 -fold at least one time point.

^b Genes downregulated $\geq 50\%$ at one time point.

Junc, *Nf-atca*, *Meca39*, *Rrg*), antioxidant enzyme genes (e.g., *Gcllc*, *Ggt*), *Pkca*, and tyrosine phosphatase genes (Fig. 1B, set 1). Early induction of several functionally similar genes (e.g., *Col6a1*, cytochrome P450 hydroxylases/oxidoreductases, *Pkc γ*) as well as heat shock proteins (*Hsp68*, *Hsp40*, *Hsp-e71*) and *Angl* was resolved at 72 h of exposure (Fig. 1B, set 2). Multiple genes with peak induction at 72 h included transcription factors and oncogenes (e.g., *c-Fos*, *Fra-1*, *Gro*), inflammation-related peptides (*Tpa*, *Pai-1*, *Il6*), growth factors and ligands (e.g., *Fgfbp1*, *amphiregulin*), apoptosis (e.g., *Bax*, murine A20), many antioxidant/detoxifying (e.g., *Ggt*, glutaredoxin, *Gstp2*) and other enzymes (e.g., *Pla2g7*, inosine 5'-phosphate dehydrogenase 2, *Mthfd2*), calcium-dependent receptor signaling components (e.g., *Mrp8*, *Calcr*), and transporters (e.g., monocarboxylate transporter 1, calcium-activated chloride channel) (Fig. 1B, sets 3 and 4). Interestingly, some genes such as *Il-6*, *RhoC*, and *Ufo* were more than 50% decreased by hyperoxia during the early time of exposure but were upregulated thereafter (Fig. 1B, set 4). Compared to corresponding baseline

expression, the greatest upregulation by hyperoxia was detected for *Mic-1* (90-fold, 72 h), *Angl* (50-fold, 24 h), *Hsp68* (32-fold, 48 h), *amphiregulin* (23-fold, 72 h), and *Fra-1* (20-fold, 72 h).

In contrast, 100 genes were significantly downregulated more than 50% at least once during exposure (Fig. 1B, sets 5 and 6). These genes encode many G-protein-dependent signal transduction elements, cytoskeletal proteins, immunoglobulins, myosin light chain, cardiac actin/troponin, and ESTs (Table 2B).

Genes differentially expressed in Nrf2^{+/+} and Nrf2^{-/-} mice after hyperoxia

ANOVA ($p < 0.05$) restricted by genotype identified 692 genes that were differentially expressed between *Nrf2^{+/+}* and *Nrf2^{-/-}* mice during hyperoxia exposure. These genotype-varied genes were then further restricted by exposure and 252 genes whose expression was significantly influenced by hyperoxia ($p < 0.05$) were elucidated. Expression kinetics of these genotype-varied, hyperoxia-

Table 2(B)
Representative genes significantly decreased ($\geq 50\%$) by hyperoxia in the lungs of wild-type (*Nrf2*^{+/+}) mice

| Name | Accession No. | Description | Classification/function |
|--|---------------|--|-------------------------------|
| Signal transduction | | | |
| <i>Grp-1</i> ^c | RU84265 | Gastrin-releasing peptide receptor | G-protein dependent signaling |
| <i>Gtpi</i> | AJ007972 | Interferon induced GTPase | G-protein dependent signaling |
| <i>Mgbbp-2</i> | AJ007970 | Murine guanylate binding protein 2 | G-protein dependent signaling |
| <i>Rad</i> | AF084466 | Ras-like GTP-binding protein, GTPase | G-protein dependent signaling |
| <i>Wnt10b</i> | U61970 | Secreted factor, protooncogene | Wnt receptor signaling |
| Cellular components | | | |
| Myosin ^c | X12972 | Myosin alkali light chain | Cytoskeleton |
| <i>Mylc2a</i> ^c | AA839903 | Myosin regulatory light chain 2 | Cytoskeleton |
| <i>Actc-1</i> | M15501 | α -Cardiac actin | Cytoskeleton |
| <i>Tncc</i> ^c | M29793 | Slow/cardiac troponin C | Cytoskeleton |
| α -actin ^c | M12347 | Skeletal α -actin | Cytoskeleton |
| <i>Tna</i> ^c | X79199 | Tetranectin, a plasminogen-binding protein with a C-type lectin domain | Extracellular matrix |
| Enzymes | | | |
| <i>Cpk-m</i> | U55772 | p170 Phosphatidylinositol 3-kinase | Kinase |
| <i>Pgam2</i> ^c | AF029843 | Phosphoglycerate mutase, muscle-specific | Mutase |
| Inflammation and immunity | | | |
| <i>Igk-v20</i> | X16678 | Ig κ light chain V-region precursor | Ig superfamily member |
| <i>Igm</i> | M80423 | Ig κ chain, putative | Ig superfamily member |
| <i>Iga</i> ^c | J00475 | Ig, secreted form | Ig superfamily member |
| <i>Car</i> | U90715 | Cell surface protein MCAR | Ig superfamily member |
| <i>Cd3r-ϵ</i> ^c | M 23376 | T cell receptor CD3 antigen, ϵ polypeptide | T cell receptor |
| <i>T3d</i> | X02339 | T3 δ -chain | T cell receptor |
| <i>Bap29</i> | X78684 | IgD B-cell receptor-associated protein | B cell receptor |
| <i>Xlp</i> | AF097632 | X-linked lymphoproliferative syndrome gene, SLAM-associated | Immune abnormality |
| <i>Ifi203</i> | AF022371 | Nuclear protein, interferon-inducible protein 203 | Nuclear protein |
| <i>Tnfc</i> | U16985 | Lymphotoxin- β | Cytokine |
| Receptors | | | |
| <i>Pgf</i> | D17433 | Prostaglandin F receptor | Hormone |
| <i>Adrb-3</i> | X72862 | β -3-Adrenergic receptor | Autonomic nerve |
| <i>Crbl1</i> | X60367 | Cellular retinal binding protein 1 | Retinol transport/metabolism |
| Others | | | |
| <i>Wsb1</i> | AF033186 | WD-40-repeat protein with a SOCS box | RNA elongation |
| <i>Gob-4</i> | AB016592 | GOB-4 in intestinal goblet cells | Secretion (?) |
| <i>Ltn-1</i> | M17818 | Major urinary protein 1 | Urinary |
| <i>Adipoq</i> | U49915 | Adipose tissue-specific glycoprotein | Adipocyte related |
| ESTs | | | |
| AW230066, AW124988, AV347370, AW12534, A690434 | | | |

^c Genes downregulated $\geq 80\%$ at least one time point.

altered genes was sorted into nine distinct patterns by *k*-means clustering (Fig. 2A), and 175 known genes (i.e., ESTs were excluded) are presented in a gene tree (Fig. 2B). The largest group of genes identified by ontology classification included genes that encode well-known or putative ARE-bearing antioxidant enzymes/redox cycle-related proteins (Table 3A). As shown in a gene tree cluster (Fig. 2D), all of those genes were overexpressed in *Nrf2*^{+/+} mice relative to *Nrf2*^{-/-} mice throughout the exposure.

Expression of many genes with no known antioxidant function also varied between *Nrf2*^{+/+} and *Nrf2*^{-/-} mice after hyperoxia (Table 3B). For example, genes encoding various enzymes (e.g., *Pkc- α* , *C62*, *Tkt*, *Ldh-2*), cytokine/chemokine receptors, and membrane transporters (e.g., *Pmp34*, *Nkcc1*) were upregulated more in *Nrf2*^{+/+} mice than in *Nrf2*^{-/-} mice. Conversely, genes encoding many

structural components (e.g., collagens, *Dy*, *Vcl*, *Myh11*) and cell growth/death proteins (e.g., *Tr21*, *Egr-2*, *Fgfbp1*) were markedly upregulated in *Nrf2*^{-/-} mice, compared to *Nrf2*^{+/+} mice.

Hyperoxia decreased genes for G-protein-linked signal proteins, including GTPI (interferon- γ -induced GTPase) and other CNC-basic leucine zipper transcription factors (NFE2, NRF3), significantly more in *Nrf2*^{+/+} mice, compared to *Nrf2*^{-/-} mice. In contrast, several chemokine/cytokine genes (e.g., *Mig*, *Mcp-2*, *Angie2*, *Pai-2*), *Wnt-4*, and *Wsb1* were downregulated more in *Nrf2*^{-/-} mice than in *Nrf2*^{+/+} mice throughout the exposure.

Overall, the array analyses elucidated several pulmonary antioxidant/detoxifying protein genes (*Aox-1*, *Ex*, *Txnrd1*, *Fil*, *Cp-2*, *Brp-12*) and non-antioxidant genes, including Tcf3 (transcription factor-3), *Lyl12* (bacteria-

binding macrophage receptor, MARCO), *Pkca*, and *Aql* (aquaporin-1), that are novel for hyperoxia-induced lung injury. Upregulation of these genes was potentiated in the

presence of *Nrf2* during the development of hyperoxic lung injury. Conversely, expression of many collagens (specifically types 1, 4, and 6 α), *Vcl*, *Cpx-1*, and *Vanin3* was more highly induced by absence of *Nrf2* in hyperoxic lungs. Venn diagram analysis identified 77 genes that varied significantly at baseline and during hyperoxia exposure ($p < 0.05$) between genotypes (see footnote in Tables 3A and 3B).

Confirmation of array results by RT-PCR and protein determination by Western blot analyses/immunohistochemistry

RT-PCR was performed for selected genes that varied markedly between *Nrf2*^{+/+} and *Nrf2*^{-/-} mice and confirmed the expression patterns of microarray analysis (Figs. 3 and 4). Protein levels of several genes were detected by Western blot analyses (Fig. 5A). Consistent with their NRF2-dependent mode of gene expression patterns, hyperoxia caused differential protein production of GSTs (α , μ), GPx2, G6PD, NQO1, pPKC α , collagen VI, HSP70 (HSP68), Krox-20 (Egr-2, Zfp-25), vinculin, and laminin-B1 in the lung after 48 or 72 h of hyperoxia (peak expressions presented in Fig. 5A). To confirm greater induction of several tyrosine phosphatase genes (e.g., *Ptpb2*, *C62*) in *Nrf2*^{+/+} mice than in *Nrf2*^{-/-} mice, Western analysis was performed with a pTyr antibody. Tyrosine phosphorylation of several proteins (approximate molecular weight 200, 120, 85, 35 kDa) was decreased by hyperoxia in *Nrf2*^{+/+} mice (Fig. 5A). In contrast, a marked increase of tyrosine phosphorylation was found in many proteins, including ~120-, ~75-, and ~45-kDa proteins, of *Nrf2*^{-/-} mice after exposure. These proteins were predicted in previous hyperoxia studies [21] as focal adhesion kinase epidermal growth factor receptor, and extracellular signal-regulated kinase.

Immunoperoxide-DAB staining (brown deposition) localized NRF2 prominently in airway epithelium (lining

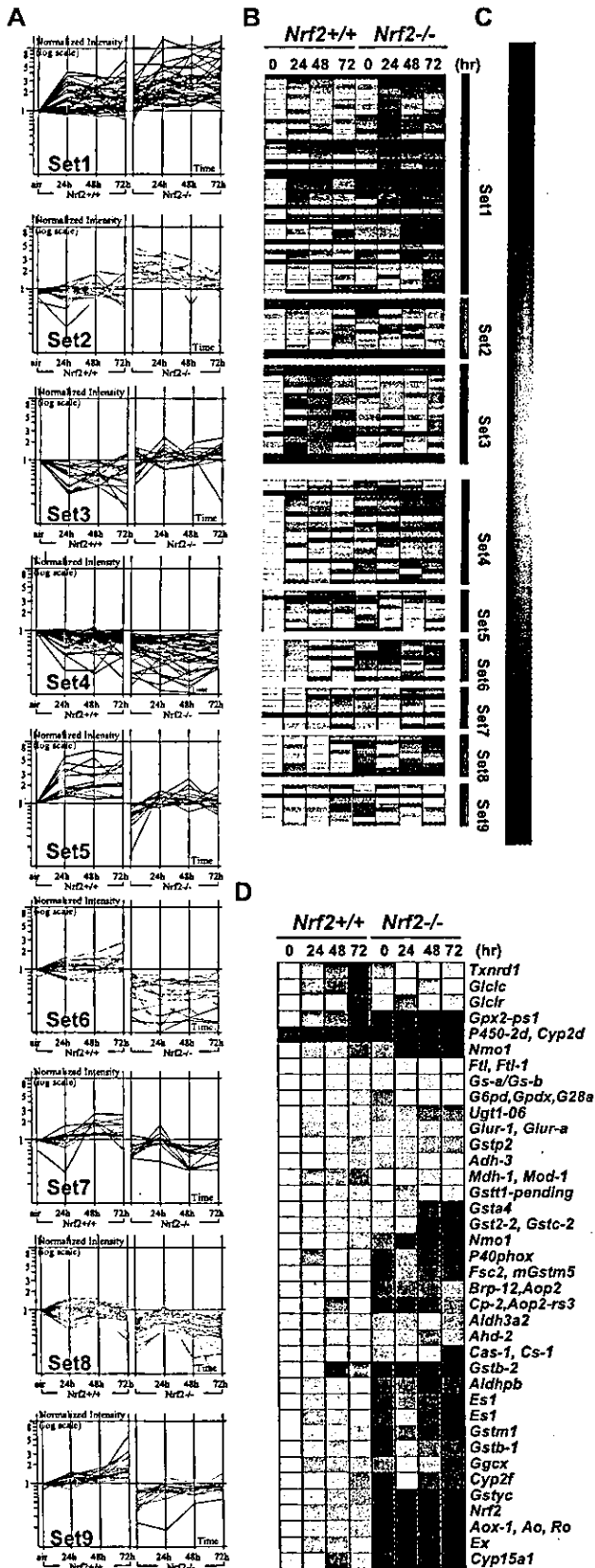


Fig. 2. (A) Nine clusters of hyperoxia-responsive genotype-variable genes ($n = 252$) between *Nrf2*^{+/+} and *Nrf2*^{-/-} mice classified based on expression patterns over time course (air and 24, 48, and 72 h O₂) by *k*-means clustering analysis. Expression level of each gene was normalized to that of air-exposed *Nrf2*^{+/+} mice and expressed as relative log ratio. (B) Gene tree clusters of genotype-varied hyperoxia-responsive genes (175 known of 252 genes) in each cluster subset. Color bar beside each cluster matches with graph color of the set in (A). (C) Color bar for expression intensity parameter of gene trees. Yellow color indicates the expression level of standard for normalization, which corresponds to the expression intensity of each gene in normal control (i.e., air-exposed *Nrf2*^{+/+} mice). Change of color from yellow to red indicates degree of upregulated intensity. Change of color from yellow to blue indicates degree of downregulated intensity. (D) Gene tree cluster of antioxidant/defense enzymes and redox-related protein genes significantly overexpressed in the lungs of *Nrf2*^{+/+} mice, compared to *Nrf2*^{-/-} mice. NRF2-regulated antioxidant/defense genes were clustered by gene tree analysis to compare time-dependent changes of gene expression levels by color in two genotypes.

Table 3 (A)

Antioxidant enzyme and redox cycle-related genes significantly ($p < 0.05$) overexpressed in the hyperoxic lungs of *Nrf2*^{+/+} mice, relative to *Nrf2*^{-/-} mice

| Name (cluster subset) | Accession No. | Description | Peak time (h)/ratio ^a |
|--|---------------|--|----------------------------------|
| Transferase | | | |
| <i>Gstp2</i> (7) ^{b,c} | X53451 | Glutathione S-transferase, $\pi 2$ | 72/2.4 |
| <i>Gstyc</i> (4) ^c | X65021 | Subunit structure GST YcYc; glutathione transferase | Downregulated/2.8 |
| <i>Gst2-2, Gstc-2</i> (8) | J03958 | Glutathione S-transferase, $\alpha 2$ (Yc2) | 72/3.9 |
| <i>Gsta4</i> (8) | L06047 | Glutathione transferase, $\alpha 4$, lung-specific | 72/4 |
| <i>Gstb-1, Gstb1</i> (9) ^c | J03952 | Glutathione S-transferase, $\mu 1$ | 48/2.3 |
| <i>Gstb-2, Gstb2</i> (4) ^c | J04696 | Glutathione S-transferase, $\mu 2$ | Downregulated/2.5 |
| <i>Fsc2, mGstm5</i> (4) ^c | J03953 | Glutathione transferase (EC 2.5.1.18) | Downregulated/1.6 |
| <i>Gstm1</i> (4) ^c | A1841270 | Glutathione S-transferase, m1 | 24/2.1 |
| <i>Gstt1</i> -pending (7) | A1843119 | Glutathione S-transferase, t1 pending | 72/1.8 |
| <i>Ugt1-06</i> (6) | U16818 | UDP glucuronosyl transferase | 24/1.7 |
| Oxidoreductase/reductase | | | |
| <i>Nmo1</i> (6) | U12961 | NAD(P)H:menadione oxidoreductase | 72/36.4 |
| <i>Txnrd1</i> (5) ^c | AB027565 | Thioredoxin reductase 1, selenocysteine | 72/3.4 |
| <i>Cp-2</i> (4) | AF093853 | 1-Cys peroxiredoxin protein 2, CP-2 | Downregulated/2.1 |
| <i>Brp-12</i> (6) | AF093857 | 1-Cys peroxiredoxin protein, CP-3 | 24/1.8 |
| Glutathione biosynthesis | | | |
| <i>Gclcr</i> (9) | U95053 | Glutamate-cysteine ligase regulatory subunit | 72/3.5 |
| <i>Gclcc</i> (5) | U85414 | γ -Glutamylcysteine synthetase, gcs heavy chain | 72/4.7 |
| <i>Gs-a/Gs-b</i> | U35456 | Glutathione synthetase type A1 | 48–72/1.5 |
| <i>Ghur-1, GluR-A</i> (9) | X57497 | Glutamate receptor 1 | 24/1.8 |
| NADPH regenerating enzyme | | | |
| <i>G6pd, Gpdx, G28a</i> (9) | Z11911 | Glucose-6-phosphate dehydrogenase | 72/1.7 |
| <i>Mdh-1, Mod-1</i> (5) | J02652 | Malate NADP oxidoreductase | 72/2 |
| Dehydrogenase | | | |
| <i>Ahd-2</i> (4) ^c | M74570 | Aldehyde dehydrogenase II | Downregulated/1.3 |
| <i>Aldh3a2</i> (4) | AV276715 | Similar to U14390 aldehyde dehydrogenase (Ahd3) | Downregulated/1.4 |
| <i>Aldhpb, Ahd2-like</i> (8) | U96401 | Aldehyde dehydrogenase Ahd2-like | 24/2.3 |
| <i>Adh-3</i> (7) | U20257 | Alcohol dehydrogenase, class IV | 72/1.9 |
| Esterase | | | |
| <i>Es1</i> (8) | AW226939 | Similar to carboxylesterase | 24/2.3 |
| <i>Ex</i> (6) | Y12887 | Carboxylesterase | 24–48/7.9 |
| <i>Ggcx</i> (8) ^c | AI507104 | Similar to vitamin-K-dependent γ -carboxylase (human) | 24–48/2 |
| Cytochrome P450 | | | |
| <i>Cyp15a1, D7ucla4</i> (7) ^c | M19319 | Cytochrome P450, 2a4, testosterone 15- α -hydroxylase | 48/13.9 |
| <i>Cyp2f</i> (4) ^c | M77497 | Cytochrome P-450 naphthalene hydroxylase | Downregulated/3.3 |
| <i>P450-2d, Cyp2d</i> (5) | M27168 | Cytochrome P450-16- α -hydroxylase | 24–72/2.2 |
| Oxidase | | | |
| <i>Gpx2-ps1</i> (7) | X91864 | Gpx2 pseudogene, selenocysteine | 72/7.24 |
| <i>Aox-1, Ao, Ro</i> (6) ^c | AB017482 | Retinal oxidase/aldehyde oxidase | 24–48/5.5 |
| <i>Fil, Fil-1</i> (7) | L39879 | Ferritin L-subunit | 48–72/1.2 |
| <i>P40phox</i> (4) | U59488 | Adaptor protein, phagocyte NADPH-oxidase activator | 72/3 |
| Catalase | | | |
| <i>Cas-1, Cs-1</i> (8) | M29394 | Catalase 1 | 24/1.3 |

^a *Nrf2*^{+/+}:*Nrf2*^{-/-} expression ratio at peak time of expression.^b *k*-means clustering subsets in Fig. 2A.^c Constitutively overexpressed genes in *Nrf2*^{+/+} mice relative to *Nrf2*^{-/-} mice ($p < 0.05$).

the main stem bronchi, small bronchioles, and terminal bronchioles) as well as in alveolar Type 2 cells and resident macrophages of normal lungs from *Nrf2*^{+/+} mice (Fig. 5B). Hyperoxia induced lung NRF2 deposition time dependently in *Nrf2*^{+/+} mice (72 h shown in Fig. 5B). Higher magnification showed intense localization of NRF2 throughout airway and alveolar epithelia and in nuclei of infiltrated macrophages after hyperoxia (arrows in Fig. 5B). NRF2 was not detected in *Nrf2*^{-/-} mice (only 72 h shown in Fig. 5B). GPx2 (Fig. 5C) and GST- α (data not shown) proteins were predominantly localized in airway/alveolar epithelia and macrophages, where NRF2 was detected, or in

smooth muscle cells lining blood vessels. Basal level of GPx2 was higher in *Nrf2*^{+/+} mice, compared to *Nrf2*^{-/-} mice. GPx2 level was highly elevated by hyperoxia in the wild-type mice, whereas marginal increase of GPx2 was detected in *Nrf2*^{-/-} mice (Fig. 5A and 5C). Microfibrillar type VI collagen, which plays a role in bridging cells with extracellular matrix, was broadly detected in bronchovascular structures in all control mice. After hyperoxia (72 h shown in Fig. 5D), type VI collagen deposition was enhanced over controls in both strains of mice. However, overall intensity of collagen staining was greater in the susceptible *Nrf2*^{-/-} mice, relative to *Nrf2*^{+/+} mice, with

Table 3 (B)
Representative known genes differentially upregulated by hyperoxia in *Nrf2*^{+/+} and *Nrf2*^{-/-} mice

| Genes expressed relatively higher in <i>Nrf2</i> ^{+/+} mice | | | Genes expressed relatively higher in <i>Nrf2</i> ^{-/-} mice | | |
|--|---------------|--|--|---------------|---|
| Name (cluster) ^a | Accession No. | Description | Name (cluster) ^a | Accession No. | Description |
| Transcription factor/DNA binding protein | | | Transcription factor/DNA binding protein | | |
| <i>Nrf2</i> (6) ^b | U70475 | p45 NF-E2-related factor 2 | <i>Egr-2</i> , <i>Krox-20</i> , <i>Zfp-25</i> (1) | M24377 | Zinc finger protein B |
| <i>Tcf-3</i> (8) | AJ223069 | TCF-3 protein | <i>Tef-3</i> (1) | X94441 | Transcription factor |
| <i>Lim1</i> (9) | Z27410 | Putative transcription regulator | <i>Lrg-21</i> (1) | U19118 | Leucine zipper protein |
| | | | <i>Orf1</i> (1) | AB019029 | Cofactor required for Sp1 transcriptional activation subunit 2 |
| | | | <i>Zfp144</i> (1) | D90085 | ORF for Mel-18 |
| | | | <i>N10</i> (2) | X16995 | Nuclear protein, hormone receptor, zinc finger protein |
| Cell death/growth/maintenance | | | Cell death/growth/maintenance | | |
| <i>Fgfbp1</i> (9) | AF065441 | FGF binding protein 1 | <i>Rtr11</i> , <i>Tr21</i> (1) | U70210 | Similar to the C-terminus of rat transcriptional activator FE65 |
| <i>Fgrp</i> , <i>Fr-1</i> (9) | U04204 | Aldose reductase-related protein | <i>Tsg6</i> (1) | U83903 | TNF-stimulated gene 6, TNF-receptor ligand |
| <i>Nr1c3</i> , <i>Ppar-γ</i> (6) ^b | U10374 | Peroxisome proliferator-activated receptor γ | <i>Tgf-β2</i> (1) | X57413 | Transforming growth factor-β 2 precursor |
| <i>Cdh15</i> (7) | AJ245402 | Cadherin, cell adhesion molecule | <i>Wisp1</i> (1) | AF100777 | Connective tissue growth factor-related protein |
| <i>β Ig-h3</i> (5) | L19932 | P68 Ig-type growth factor, cell adhesion inhibitor | <i>Flk-1</i> (1) | X70842 | FLK endothelial cell growth factor |
| <i>N1</i> (9) | M14220 | Neuroleukin, lymphokine, growth factor | <i>Aigf</i> , <i>Fgf-8</i> (1) | D12483 | Fibroblast growth factor |
| | | | <i>Hsp68</i> (1) ^c | M12571 | 68-kDa heat shock protein |
| | | | Extracellular matrix/cytoskeleton | | |
| | | | <i>Coll1a1</i> (1) | U03419 | Procollagen α 1 (I) |
| | | | <i>Col6a-2</i> (1) | Z18272 | Collagen α 2 (VI) |
| | | | <i>Coll18a1</i> (1) ^c | L22545 | Collagen α 1 (XVIII) |
| | | | <i>Coll13a1</i> (1) ^c | U30292 | Collagen α 1 (XIII) |
| | | | <i>Dy</i> , <i>Mer</i> , <i>Merosin</i> (1) ^c | U12147 | Laminin-2 m-chain; merosin α2 chain; merosin m-chain |
| | | | <i>Lamb-1</i> (1) ^c | X05212 | Laminin B1 |
| | | | <i>Eln</i> (1) | U08210 | Tropoelastin |
| | | | <i>Smsmo</i> (1) | AJ010305 | Smoothelin L1, large isoform |
| | | | <i>Fbln1</i> (1) | X70853 | BM-90/fibulin |
| | | | <i>Fbln2</i> (1) ^c | X75285 | Fibulin-2 |
| | | | <i>Vcl</i> (1) | L18880 | Vinculin |
| | | | <i>Actv3</i> (3) | X13297 | Actin, α2, smooth muscle, aorta |
| | | | <i>Act-4</i> , <i>Acta3</i> (1) | U20365 | Smooth muscle γ-actin |
| | | | <i>Fbn-1</i> (1) ^c | L29454 | Fibrillin |
| | | | <i>Myh11</i> (1) | D85923 | Myosin heavy chain 11, smooth muscle |
| Signal transduction | | | Signal transduction | | |
| <i>Strap</i> (6) | AF096285 | TGF-β receptor-associated protein | <i>Chrm-4</i> , <i>M4</i> (3) | X63473 | m4 muscarinic acetylcholine receptor |
| <i>Bet</i> , <i>Prpb2</i> (9) | D83203 | Receptor-type protein tyrosine phosphatase | <i>Achr-2</i> , <i>Acrb</i> (3) | M14537 | Acetylcholine receptor β subunit |

(continued on next page)